arXiv:1402.6916v1 [cond-mat.soft] 27 Feb 2014

Electrostatic interaction between colloidal particles trapped at an electrolyte interface

Arghya Majee,* Markus Bier,† and S. Dietrich

Max-Planck-Institut für Intelligente Systeme,

Heisenbergstr. 3, 70569 Stuttgart, Germany,

and Institut für Theoretische Physik IV, Universität Stuttgart,

Pfaffenwaldring 57, 70569 Stuttgart, Germany

(Dated: February 28, 2014)

Abstract

The electrostatic interaction between colloidal particles trapped at the interface between two immiscible electrolyte solutions is studied in the limit of small inter-particle distances. Within an appropriate model exact analytic expressions for the electrostatic potential as well as for the surface and line interaction energies are obtained. They demonstrate that the widely used superposition approximation, which is commonly applied to large distances between the colloidal particles, fails qualitatively at small distances and is quantitatively unreliable even at large distances. Our results contribute to an improved description of the interaction between colloidal particles trapped at fluid interfaces.

*Electronic address: majee@is.mpg.de

†Electronic address: bier@is.mpg.de

I. INTRODUCTION

Colloidal particles, trapped at fluid interfaces by adsorption energies much larger than the thermal energy, can form effectively two-dimensional colloidal monolayers [1]. During the last two decades these systems have received significant attention both in basic research as well as in applied sciences. On one hand, these monolayers serve as model systems for studying effective interactions, phase behaviors, structures, and the dynamics of condensed matter in reduced dimensionality [2–8]. On the other hand, self-assembled colloidal monolayers find applications in optical devices, molecular electronics, emulsion stabilization processes, and as templates in the fabrication of new micro- and nanostructured materials. Therefore, a reliable description of the lateral inter-particle interaction at all distances r, which governs the structure formation of colloids at fluid interfaces, is of primary importance.

In his pioneering work Pieranski [1] showed that the electrostatic *repulsion* of charged colloids at such interfaces is dominated by a long-ranged dipole-dipole interaction, due to an asymmetric counterion distribution in the two adjacent media, in addition to the screened Coulomb interaction also present in bulk systems. Later both the power-law and the exponential contributions have been calculated within the framework of linearized Poisson-Boltzmann theory assuming point-like particles [9]. It turned out that, whereas the interaction energy for charged particles always decays asymptotically $\propto 1/r^3$, the prefactor depends on whether the interaction originates from charges on the polar [1, 10] or on the apolar [11, 12] side of the fluid interface. In addition there are experimental indications of an *attractive* long-ranged lateral interaction which cannot be interpreted in terms of a van der Waals force [13, 14]. Attempts were made to explain it in terms of a deformation-induced capillary interaction, but a complete and final picture has not yet been reached [15–18]. Here, we focus on the electrostatic contribution to the interaction.

Whereas Pieranski's work has been extended in numerous directions, almost all subsequent studies have discussed exclusively the case of colloidal particles being far away from each other. In this asymptotic limit the superposition approximation has been assumed to be reliable, according to which one approximates the actual electrostatic potential (or interfacial deformation) for a pair of particles by the sum of the potentials (or deformations) of the two single particles. However, for a dense system or during aggregation, particles can come close to each other such that this superposition approximation is no longer justified.

For the deformation induced attractive part of the interaction, the validity of this approximation has been discussed for both large [16, 18, 19] and small [20] separations. But so far for the repulsive electrostatic interaction no investigations of small-distance deviations from the superposition approximation have been reported, although a systematic multipole expansion of the electrostatic potential around a single inhomogeneously charged particle trapped at an interface is available [21].

Here, we assess the quality of the superposition approximation for the electrostatic interaction between two colloidal particles floating close to each other at an electrolyte interface by considering a simplified problem (see Fig. 1) which offers the possibility to obtain exact analytic expressions. Accordingly, first, the interface is assumed to be planar, i.e., no deformations of the fluid interface are considered, which are typically of the order of nanometers for micron-sized particles [13, 14, 22]. Second, due to the small particle-particle distances to be studied, the curvature of the colloidal particles is ignored in the spirit of a Derjaguin approximation [23] by considering the effective interaction between two charged, planar, and parallel walls. Third, a liquid-particle contact angle of 90° is assumed; this value is encountered for actual systems [24]. We have derived an exact analytic expression for the electrostatic potential of this model within linearized Poisson-Boltzmann theory, which is then used to calculate the surface interaction energies per total surface area and the line interaction energy per total length of the two three-phase contact lines (Fig. 1). The main result is the observation of significant deviations between the exact values of these quantities and those obtained within the superposition approximation, both at small and even at large distances (see Fig. 2).

II. ELECTROSTATIC POTENTIAL

Consider a three-dimensional Cartesian coordinate system such that the two charged planar walls, which mimic the colloidal particles, are located at $z = \pm L$ and the fluid interface is at $x = 0$ (Fig. 1(b)). The electrolyte solution present at $x > 0$ ($x < 0$) is denoted as medium "1" ("2"). For simplicity here we consider binary monovalent electrolytes only, i.e., there are only two ionic species of opposite sign like Na^+ and Cl^-. Generically the ions and the molecules are coupled such that the molecular and ion number densities vary on the scale of the bulk correlation length which is much smaller than the Debye length

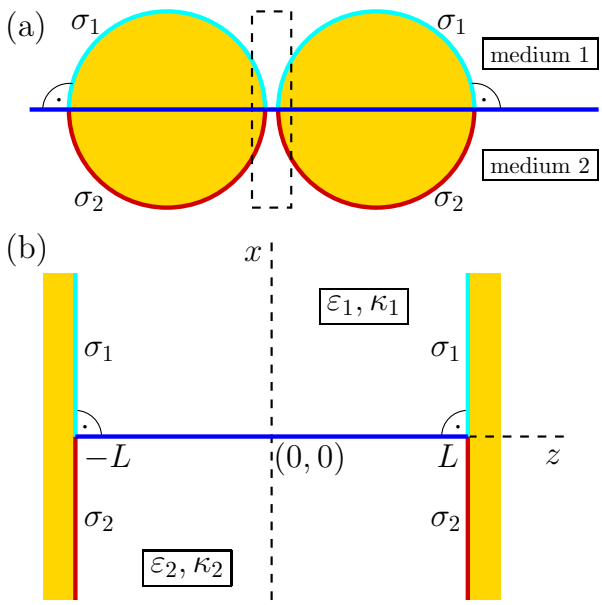

FIG. 1: (a) Cross section of two identical spherical particles trapped at a fluid interface (horizontal blue line) close to each other and with contact angle 90°. (b) Magnified view of the boxed region in (a). The two adjacent fluids ("1", located at $x > 0$, and "2", located at $x < 0$) forming the interface have permittivities ε_1, ε_2 and inverse Debye lengths κ_1, κ_2, respectively. Since the surface-to-surface distance between the particles is small compared to their radii, the particle surfaces can be approximated by planes located at $z = \pm L$ which carry charge densities σ_1 and σ_2 at the surfaces in contact with fluid "1" and "2", respectively. According to the model the fluid structures vary steplike at the surfaces and at the interface.

which sets the length scale for the variation of the charge density [25]. Thus the number densities in both media vary only close to the walls or to the fluid interface at distances of the order of the bulk correlation length, which, away from critical points, is of the order of the size of the fluid molecules and of the ions and falls below the length scale to be considered here. Accordingly, the permittivity ε_1 (ε_2) and the inverse Debye length κ_1 (κ_2) in medium "1" ("2") are uniform where $\kappa_i = (2I_i e^2/(\varepsilon_i k_B T))^{1/2}$, $i \in \{1, 2\}$, with bulk ionic strength I_i (which is the bulk number density of each ionic species in medium i), Boltzmann constant k_B, temperature T, and elementary charge $e > 0$. The two walls are assumed to be chemically identical such that the surface charge densities at both half-planes in contact with medium "1" ("2") are given by σ_1 (σ_2). The local charge density of the ions is *not* uniform in media "1" or "2" because this quantity varies on the scale of the Debye lengths,

which are typically much larger than molecular sizes. Since the slab formed by the two walls at $z = \pm L$ is a model of the space in between two colloidal particles trapped at the fluid interface, it is appropriate to describe the ions within a grand canonical ensemble, the reservoirs of which are given by the bulk electrolyte solutions far away from the fluid interface. Within a simple density functional theory, which (i) considers uniform solvents in the upper and the lower half space, (ii) assumes low ionic strength in the bulk (which facilitates the description of the ions as point-like particles), and (iii) describes deviations of the ion densities from the bulk ionic strengths only up to quadratic order, one derives the linearized Poisson-Boltzmann (PB) equation $(\Delta - \kappa_i^2)\Phi_i = 0$ to be fulfilled by the electrostatic potential $\Phi_i(x, z)$ in medium $i \in \{1, 2\}$. The corresponding boundary conditions are: (i) the electrostatic potential should remain finite for $x \to \pm\infty$, (ii) the electrostatic potential and the normal component of the electric displacement field at the fluid interface should be continuous, i.e., $\Phi_1(x = 0^+, z) = \Phi_2(x = 0^-, z)$ and $\varepsilon_1 \partial_x \Phi_1(x = 0^+, z) = \varepsilon_2 \partial_x \Phi_2(x = 0^-, z)$, and (iii) due to global charge neutrality the normal component of electric displacement field at the walls correspond to the surface charge densities, i.e., $\varepsilon_i \partial_z \Phi_i(x, z = \pm L) = \pm\sigma_i$. It is important to note that in our model the fluids are confined to the space between the two walls such that outside the fluid slab the electric field vanishes.

In order to determine the electrostatic potential we first split the whole problem into three sub-problems (see appendix A): (i) only the fluid interface is present in the absence of any walls, (ii) two charged walls with homogeneous surface charge densities σ_1 and the uniform medium "1" in between, and (iii) two charged walls with homogeneous surface charge densities σ_2 and the uniform medium "2" in between. By adding the solution of problem (ii) and the solution of problem (i) for the upper half-space and by adding the solution of problem (iii) and the solution of problem (i) for the lower half-space, one obtains potentials in the two media which satisfy all the boundary conditions listed above except the continuity of the potential at the interface. In order to fulfill also the latter one, we construct a correction function which (i) is a solution of the linearized PB equation, (ii) keeps all boundary conditions unchanged which are already satisfied, and (iii) leads to continuity of the potential at the interface. This can be achieved by means of 2D Fourier transform or Fourier series expansions [26]. The final expression for the *e*xact electrostatic potential

(denoted by superscript "e") reads

$$\begin{aligned}\Phi_i^e(x,z) =& \Phi_{bi} + \sum_{j\in\{1,2\}}^{j\neq i} \frac{(-1)^j \kappa_j \varepsilon_j \Phi_D}{\kappa_1\varepsilon_1 + \kappa_2\varepsilon_2} e^{-\kappa_i|x|} \\ &+ \Phi_i^{(0)} \frac{\cosh(\kappa_i z)}{\sinh(\kappa_i L)} + \sum_{j\in\{1,2\}}^{j\neq i} \frac{C_{ij}^{(0)}(L) e^{-a_i^{(0)}(L)|x|}}{2} \\ &+ \sum_{j\in\{1,2\}}^{j\neq i} \sum_{n=1}^{\infty} C_{ij}^{(n)}(L) e^{-a_i^{(n)}(L)|x|} \cos\left(\frac{n\pi z}{L}\right), \end{aligned} \tag{1}$$

where the explicit dependences of $\Phi_i^{(0)}$, $a_i^{(n)}(L)$, and $C_{ij}^{(n)}(L)$ on n, L, and the type of media i and j are given in appendix A. The electrostatic bulk potential Φ_{bi} is defined as $\Phi_{b1} = 0$ and $\Phi_{b2} = \Phi_D$, with the Donnan potential (or Galvani potential difference [27]) Φ_D between medium "2" and medium "1", which originates from the differences of the solubilities of the ions in the two media [28].

The first two terms on the right-hand side of Eq. (1) together represent the effect of the fluid interface in the absence of walls (sub-problem (i)) which corresponds to the limit $L \to \infty$ at any fixed position z. The third term describes the electrostatic potential of two uniformly and equally charged walls in the presence of a uniform electrolyte solution in between (sub-problem (ii) or (iii)). According to Eq. (1), up to the constant Φ_{bi}, $\Phi_i^e(x,z)$ reduces to the third term in the limit $|x| \to \infty$, i.e., far away from the fluid interface. The fourth and the fifth term in Eq. (1) correspond to the correction function which describes the contact of the walls with the fluid interface. Due to the symmetry of the problem, $\Phi_i(x,z)$ has to be an even function of z, and $\Phi_2(-\infty,z) - \Phi_1(\infty,z) = \Phi_D$ for any fixed position z in the limit of large wall separations $L \to \infty$. $\Phi_i^e(x,z)$ exhibits these properties.

By adding the electrostatic potentials of two single walls, each in contact with the fluid interface in a semi-infinite geometry with respect to z, one obtains the superposition approximation (denoted by superscript "s")

$$\begin{aligned}\Phi_i^s(x,z) =& 2\Phi_{bi} + \sum_{j\in\{1,2\}}^{j\neq i} \frac{2(-1)^j \kappa_j \varepsilon_j \Phi_D}{\kappa_1\varepsilon_1 + \kappa_2\varepsilon_2} e^{-\kappa_i|x|} \\ &+ 2\Phi_i^{(0)} \cosh(\kappa_i z) e^{-\kappa_i L} \\ &+ \sum_{j\in\{1,2\}}^{j\neq i} \int_0^{\infty} dq\; C_{ij}^s(q) \cos(qL)\cos(qz) e^{-\sqrt{q^2+\kappa_i^2}|x|}. \end{aligned} \tag{2}$$

The explicit expression for $C^s_{ij}(q)$ is given in appendix A. A comparison between the exact electrostatic potential $\Phi^e_i(x,z)$ and the superposition approximation $\Phi^s_i(x,z)$ at the plane of interface ($x = 0$) is displayed in Fig. 5 in the appendix. Moreover, $\Phi^s_i(x,z)$ does not satisfy the boundary condition which relates the electric displacement field at the walls to the surface charge densities and $\Phi^s_2(-\infty,z) - \Phi^s_1(\infty,z) \neq \Phi_D$ for any fixed position z in the limit of large wall separations $L \to \infty$.

III. SURFACE AND LINE INTERACTIONS

With the electrostatic potential given, the corresponding grand canonical potential can also be determined both exactly as well as within the superposition approximation. After subtracting the bulk free energy, the surface and interfacial tensions, and the line tension contributions from the grand potential one obtains the L-dependent part of the grand potential,

$$\Delta\Omega(L) = A_1\omega_{\gamma,1}(L) + A_2\omega_{\gamma,2}(L) + \ell\omega_\tau(L), \tag{3}$$

for the walls being a distance $2L$ apart, where A_1 and A_2 are the total areas of the two walls in contact with medium "1" and "2", respectively, and ℓ is the total length of the three-phase contact lines formed by medium "1", medium "2", and the walls; by construction $\Delta\Omega(L \to \infty) \to 0$. The surface interaction energy per total surface area A_i ($\omega_{\gamma,i}$) in contact with medium $i \in \{1,2\}$ is exactly (superscript "e") given by

$$\omega^e_{\gamma,i}(L) = \frac{\sigma_i^2}{2\kappa_i\varepsilon_i}\left(\coth(\kappa_i L) - 1\right), \tag{4}$$

and within the superposition approximation (superscript "s") by

$$\omega^s_{\gamma,i}(L) = \frac{\sigma_i^2}{2\kappa_i\varepsilon_i}\left(2e^{-\kappa_i L}\cosh(\kappa_i L) - 1\right). \tag{5}$$

According to Eqs. (4) and (5), varying σ_i and ε_i influences only the amplitude of $\omega_{\gamma,i}$ whereas its decay rate is solely determined by κ_i. For large wall separations one has $\omega^e_{\gamma,i}(\kappa_i L \gg 1) \simeq \frac{\sigma_i^2}{\kappa_i\varepsilon_i}e^{-2\kappa_i L}$ and $\omega^s_{\gamma,i}(\kappa_i L \gg 1) \simeq \frac{\sigma_i^2}{2\kappa_i\varepsilon_i}e^{-2\kappa_i L}$, i.e., the superposition approximation correctly predicts the exponential decay in the large distance limit but, in contrast to common expectations, the corresponding prefactor is too small by a factor of 2. Moreover, the superposition approximation is qualitatively wrong for small wall separations (but still

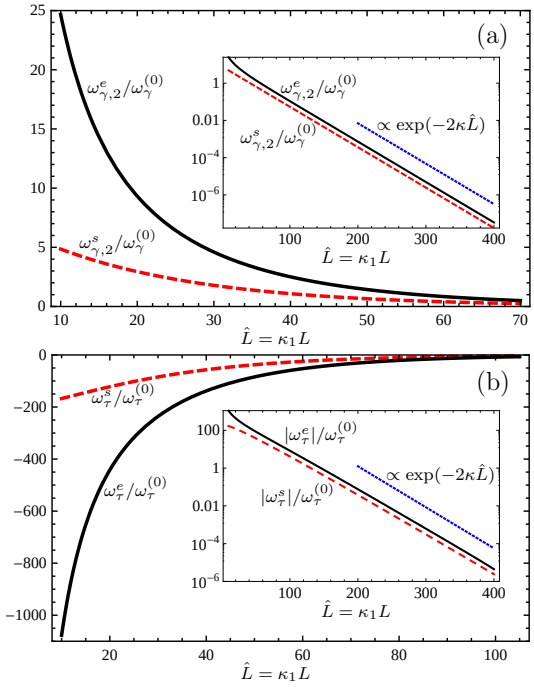

FIG. 2: (a) Comparison between the exact expression (superscript "e", black solid lines, see Eq. (4)) and the corresponding superposition approximation (superscript "s", red dashed lines, see Eq. (5)) of the surface interaction energy $\omega_{\gamma,2}(L)$ per total surface area of contact between the walls and medium "2" in units of $\omega_\gamma^{(0)} = \sigma_1^2/(\kappa_1\varepsilon_1)$ as a function of $\hat{L} = \kappa_1 L$. Typical experimental values for the parameter ratios $\kappa = \kappa_2/\kappa_1 = 0.025$, $\varepsilon = \varepsilon_2/\varepsilon_1 = 0.025$, and $\sigma = \sigma_2/\sigma_1 = 0.1$ have been chosen for the plots [13, 14, 29–31]. Obviously $\omega^e_{\gamma,2}(L)$ and $\omega^s_{\gamma,2}(L)$ differ significantly at small distances, but even in the limit of large wall separations the superposition approximation is too small by a factor of 2 (see the offset between the two curve in the inset). A similar deviation is obtained for $\omega_{\gamma,1}(L)$, but due to its very small magnitude ($\approx 10^{-10} \times \omega_{\gamma,2}(L)$, for the above parameter choices) it is not shown here (see Fig. 6 in the appendix). (b) Comparison of the exact expression (superscript "e", black solid lines) and the superposition approximation (superscript "s", red dashed lines) of the effective line interaction energy $\omega_\tau(L)$ per total length of the three-phase contact lines between media "1" and "2" and the walls in units of $\omega_\tau^{(0)} = \sigma_1^2/(\kappa_1^2\varepsilon_1)$ as a function of $\hat{L}$ (see appendix C for explicit expressions). In addition to the same parameters σ, ε, and κ as in panel (a) the Donnan potential (Galvani potential difference) $\Phi_D/\Phi_1^{(0)} = 1.3$ is used. As for the surface interaction potential in panel (a), the superposition approximation of the line interaction potential deviates qualitatively from the exact result at small wall separations and its absolute value at large distances is too small by a factor of 2.

large on the molecular scale), because the exact surface interaction potential diverges in this limit as $\omega^e_{\gamma,i}(\kappa_i L \ll 1) = \frac{\sigma_i^2}{2\kappa_i\varepsilon_i}\left[\frac{1}{\kappa_i L} - 1 + \frac{\kappa_i L}{3} + \mathcal{O}((\kappa_i L)^3)\right]$, whereas the superposition approximation stays finite: $\omega^s_{\gamma,i}(\kappa_i L \ll 1) = \frac{\sigma_i^2}{2\kappa_i\varepsilon_i}\left[1 - 2\kappa_i L + \mathcal{O}((\kappa_i L)^2)\right]$. Thus the superposition approximation underestimates $\omega_{\gamma,i}$ for all L. Since for dilute aqueous electrolyte solutions of, e.g., 1 mM ($\approx 0.0006\,\mathrm{nm}^{-3}$) ionic strength the Debye length ($1/\kappa_i \gtrsim 10\,\mathrm{nm}$) is much larger than typical molecular size (e.g., $L = 1\,\mathrm{nm}$), the exact surface interaction $\omega^e_{\gamma,i}(L)$ and the corresponding superposition approximation $\omega^s_{\gamma,i}(L)$ differ by at least one order of magnitude: $\omega^e_{\gamma,i}(L)/\omega^s_{\gamma,i}(L) \simeq 1/(\kappa_i L) \gtrsim 10$. Figure 2(a) displays a comparison between the exact result (black solid lines) and the superposition approximation (red dashed lines) for a set of typical experimental values for the ratios $\sigma = \sigma_2/\sigma_1$, $\kappa = \kappa_2/\kappa_1$, and $\varepsilon = \varepsilon_2/\varepsilon_1$.

The line interaction potential $\omega_\tau(L)$ per total length of the three-phase contact line between media "1" and "2" and the walls has been calculated from Eqs. (1) and (2) (see appendix C for explicit expressions). A comparison between the exact result $\omega^e_\tau(L)$ and the corresponding superposition approximation $\omega^s_\tau(L)$ is displayed in Fig. 2(b). Similar to the surface interaction potentials, $\omega^s_\tau(L)$ differs significantly from the exact result $\omega^e_\tau(L)$ at small wall separations $2L$. For large values of L, its absolute value is too small by a factor of 2, like the surface contribution.

IV. DISCUSSION

By considering a slab geometry, we have investigated the electrostatic interaction between two colloidal particles at close proximity trapped at the interface of two immiscible electrolyte solutions. In our calculations, we have considered the charge density at the surface of the colloids to be constant, forming a boundary condition. However, in actual systems the situation is slightly different. When two particles approach each other the electrostatic potential becomes deeper in the region between the particles. Due to that certain charged molecular surface groups recombine in order to adjust the electrostatic potential. Such a process can better be described by a charge regulation model [23]. Keeping in mind the actual complexity of the system considered here, we briefly discuss the implications of charge regulation by focusing on a simpler system which consists of an electrolyte between two charged walls without a liquid-liquid interface in between. For such a system, the electrostatic potential with a surface charge density $\sigma_{wi}(L)$ at the two walls (which is constant

for any fixed L) is given by $\Phi^e_{wi} = \frac{\sigma^e_{wi}(L)}{\kappa_{wi}\varepsilon_{wi}} \frac{\cosh \kappa_{wi} z}{\sinh \kappa_{wi} L}$ for the *e*xact calculation (see Eqs. (A3) and (A4) in the appendix) and by $\Phi^s_{wi} = \frac{2\sigma^s_{wi}(L)}{\kappa_{wi}\varepsilon_{wi}} e^{-\kappa_{wi} L} \cosh(\kappa_{wi} z)$ within the *s*uperposition approximation (see the first terms in Eqs. (A21) and (A22) in the appendix). Here the subscript "*wi*" stands for the system *w*ithout *i*nterface and the quantities σ_{wi}, κ_{wi}, and ε_{wi} indicate, respectively, the surface charge density at the walls, the inverse Debye length, and the permittivity of the medium between the two planes in the absence of the horizontal interface. The dependence of the surface charge densities $\sigma^e_{wi}(L)$ and $\sigma^s_{wi}(L)$ on L originates from the charge regulation (see appendix E). Inserting these expressions for the electrostatic potential into Eq. (B24) in the appendix and using the fact that $D_x(\mathbf{r})$ vanishes in the absense of a liquid-liquid interface as it is the case here, leads to the following surface interaction energies per total surface area of both walls:

$$\omega^e_{\gamma,wi}(L) = \frac{\left(\sigma^e_{wi}(L)\right)^2}{2\kappa_{wi}\varepsilon_{wi}} \left(\coth(\kappa_{wi} L) - 1\right) \tag{6}$$

and

$$\omega^s_{\gamma,wi}(L) = \frac{\left(\sigma^s_{wi}(L)\right)^2}{2\kappa_{wi}\varepsilon_{wi}} \left(2e^{-\kappa_{wi} L} \cosh(\kappa_{wi} L) - 1\right). \tag{7}$$

We note that Eqs. (6) and (7) are identical to Eqs. (4) and (5), respectively, except the fact that here the surface charge density varies with the thickness L of the slab.

We discuss the two limiting cases of small and large L separately. In the limit $\kappa_{wi} L \ll 1$ one has $\sigma^e_{wi}(L) \simeq -\mathrm{sign}(q) e\sqrt{2nKL}$ for the exact calculation (Eq. (E9) in the appendix) and $\sigma^s_{wi}(L)$ is constant for the superposition approximation (see appendix E). K (with units 1/volume) is the equilibrium constant for the association-dissociation reaction of the surface groups, n denotes the total number of surface sites per cross-sectional area where a dissociation reaction can take place, and q is the valency of the solvated ions due to the dissociation reaction at the wall surface (appendix E). This implies $\omega^e_{\gamma,wi}(L \to 0) = \frac{e^2 nKL}{\kappa_{wi}\varepsilon_{wi}} \left[\frac{1}{\kappa_{wi} L} - 1 + \frac{\kappa_{wi} L}{3} + \mathcal{O}((\kappa_{wi} L)^3)\right]$ which is nonzero for $L = 0$. On the other hand, the nonzero and finite limiting value $\sigma^s_{wi}(L \to 0) \neq 0$ within the superposition approximation is clearly unphysical because the charge density is expected to decrease upon decreasing the inter-particle separation distance L. If by fiat, in order to avoid this unphysical feature, in Eq. (7) we replace $\sigma^s_{wi}(L)$ by $\sigma^e_{wi}(L)$, in the limit of small L one finds $\omega^s_{\gamma,wi}(L \to 0) = \frac{e^2 nKL}{\kappa_{wi}\varepsilon_{wi}} \left[1 - 2\kappa_{wi} L + \mathcal{O}((\kappa_{wi} L)^2)\right]$, which vanishes for $L \to 0$. In the opposite limit, i.e., for

$\kappa_{wi}L \gg 1$, one finds $\omega^e_{\gamma,wi} \simeq \dfrac{\left(\sigma^e_{wi}(L)\right)^2}{\kappa_{wi}\varepsilon_{wi}} e^{-2\kappa_{wi}L}$ and, by using the same replacement as above, $\omega^s_{\gamma,wi} \simeq \dfrac{\left(\sigma^e_{wi}(L)\right)^2}{2\kappa_{wi}\varepsilon_{wi}} e^{-2\kappa_{wi}L} = \dfrac{\omega^e_{\gamma,wi}}{2}$ with $\sigma^e_{wi}(L)$ given by Eq. (E8) in the appendix. Thus for the simple slab system without a liquid-liquid interface, but with charge regulation, the exact calculation and the superposition approximation are also in disagreement by a factor of 2 in the large separation limit and they differ qualitatively in the small separation limit. For the more complicated system with a liquid-liquid interface, we can expect these discrepancies to persist.

V. CONCLUSION

Within a continuum model of two parallel plates with two different electrolyte solutions in between forming a liquid-liquid interface, we have derived exact expressions for the electrostatic potential as well as for the effective surface and the line interaction potentials. The comparison between the exact results and the corresponding expressions within the superposition approximation reveals that the latter underestimates these quantities qualitatively at short distances and quantitatively even at large distances. Depending on the specific experimental system, the difference at small distances can be significant. The issue whether the deviations at large distances persist for a spherical geometry is left for future investigations. We expect our results to improve the description of the effective interaction between colloidal particles trapped at fluid interfaces, which plays an important role, e.g., in the formation of two-dimensional colloidal aggregates.

Acknowledgments

Helpful discussions with Alois Würger are gratefully acknowledged.

Appendix A: Electrostatic Potential

1. Exact solution

In order to obtain the electrostatic potential for the planar geometry shown in Fig. 1(b) (see also Fig. 3(a)), the linearized Poisson-Boltzmann (Debye-Hückel) equation is solved in

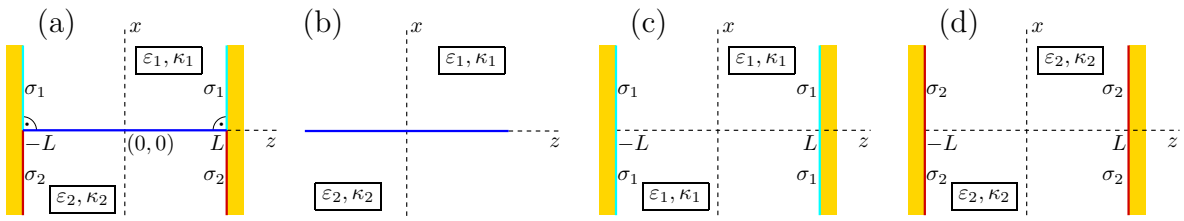

FIG. 3: (a) Slit of width $2L$ confined between two planar walls in the presence of an interface (solid blue line) between two electrolytes "1" and "2" characterized by permittivities ε_1, ε_2 and inverse Debye lengths κ_1, κ_2, respectively. In order to calculate the electrostatic potential we divide the problem in three sub-problems: (i) two adjacent electrolytes "1" and "2" separated by an interface at $x = 0$ in the absence of any walls (b), (ii) two homogeneous walls at $z = \pm L$ carrying charge densities σ_1 with the uniform electrolyte "1" in between (c), and (iii) two homogeneous walls at $z = \pm L$ carrying charge densities σ_2 with the uniform electrolyte "2" in between (d).

the two adjacent media with the following boundary conditions: (i) the potential remains finite for $x \to \pm\infty$, (ii) the electrostatic potential and the normal component of the electric displacement field are continuous at the fluid interface, i.e., $\Phi_1(x = 0^+, z) = \Phi_2(x = 0^-, z)$ and $\varepsilon_1 \partial_x \Phi_1(x = 0^+, z) = \varepsilon_2 \partial_x \Phi_2(x = 0^-, z)$, and (iii) the normal component of the electric displacement field at the walls correspond to the surface charge densities, i.e., $\varepsilon_i \partial_z \Phi_i(x, z = \pm L) = \pm\sigma_i$. In order to obtain such a solution we split the problem first into three sub-problems (Figs. 3(b)-(d)): (i) only the fluid interface is present in the absence of any walls, (ii) two charged walls with homogeneous surface charge densities σ_1 and the uniform medium "1" in between, and (iii) two charged walls with homogeneous surface charge densities σ_2 and the uniform medium "2" in between. The solution of sub-problem (i) will be denoted by $\bar{\Phi}_i(x)$ and the solutions of sub-problems (ii) and (iii) will be denoted by $\Psi_1(z)$ and $\Psi_2(z)$, respectively.

a. Solution of sub-problem (i)

For two electrolyte solutions forming an interface at $x = 0$ in the absence of any walls, the potential can be calculated by solving

$$\Delta\bar{\Phi}_1(x) - \kappa_1^2 \bar{\Phi}_1(x) = 0, \qquad (x > 0), \tag{A1a}$$

$$\Delta(\bar{\Phi}_2(x) - \Phi_D) - \kappa_2^2 (\bar{\Phi}_2(x) - \Phi_D) = 0, \qquad (x < 0), \tag{A1b}$$

with $\Delta = d^2/dx^2$ and Φ_D denoting the Donnan potential (Galvani potential difference). The solutions of these equations can be written as

$$\bar{\Phi}_1(x) = Ae^{-\kappa_1 x} + Be^{\kappa_1 x},$$
$$\bar{\Phi}_2(x) = \Phi_D + Ce^{-\kappa_2 x} + De^{\kappa_2 x}.$$

The boundary conditions $\bar{\Phi}_1(x \to \infty) \to 0$ and $\bar{\Phi}_2(x \to -\infty) \to \Phi_D$ lead to $B = C = 0$. The integration constants A and D can be obtained by using the boundary conditions that both the potential and the electric displacement field are continuous at the interface (i.e., at $x = 0$). This leads to

$$\bar{\Phi}_1(x) = \frac{\kappa_2\varepsilon_2\Phi_D}{\kappa_1\varepsilon_1 + \kappa_2\varepsilon_2}e^{-\kappa_1 x}, \tag{A2a}$$
$$\bar{\Phi}_2(x) = \Phi_D\left(1 - \frac{\kappa_1\varepsilon_1}{\kappa_1\varepsilon_1 + \kappa_2\varepsilon_2}e^{\kappa_2 x}\right). \tag{A2b}$$

b. Solutions of sub-problems (ii) and (iii)

For two homogeneously charged walls at $z = \pm L$ with surface charge densities σ_1 and uniform medium "1" in between, the electrostatic potential is given by

$$\Delta\Psi_1(z) - \kappa_1^2\Psi_1(z) = 0,$$

where $\Delta = d^2/dz^2$. The solution of this equation reads

$$\Psi_1(z) = Ae^{-\kappa_1 z} + Be^{\kappa_1 z}.$$

The integration constants A and B are determined by the boundary condition that the electric displacement field is equal to the charge density at the two walls. This leads to

$$-\kappa_1 Ae^{\kappa_1 L} + \kappa_1 Be^{-\kappa_1 L} = -\frac{\sigma_1}{\varepsilon_1},$$
$$-\kappa_1 Ae^{-\kappa_1 L} + \kappa_1 Be^{\kappa_1 L} = \frac{\sigma_1}{\varepsilon_1},$$

with the solution $A = B = \sigma_1/\left(2\kappa_1\varepsilon_1\sinh(\kappa_1 L)\right)$ so that

$$\Psi_1(z) = \frac{\sigma_1}{\kappa_1\varepsilon_1}\frac{\cosh(\kappa_1 z)}{\sinh(\kappa_1 L)}. \tag{A3}$$

Sub-problem (iii) can be solved similarly leading to

$$\Psi_2(z) = \frac{\sigma_2}{\kappa_2\varepsilon_2}\frac{\cosh(\kappa_2 z)}{\sinh(\kappa_2 L)}. \tag{A4}$$

c. Construction of a correction function and the final solution

In view of the linear nature of the Debye-Hückel equation, one can add the solution of problem (ii) and the solution of problem (i) for the upper half-space, and the solution of problem (iii) and the solution of problem (i) for the lower half-space in order to obtain solutions in each media which are also solutions of the Debye-Hückel equation. The sum $\bar{\Phi}_i(x) + \Psi_i(z)$ fulfills almost all boundary conditions for the electrostatic potential except continuity at the interface; although $\bar{\Phi}_i$ fulfills it, Ψ_i violates it. In order to rectify this, we construct a correction function $c_i(x, z)$ which has the following properties: (i) $c_i(x, z)$ is a solution of the Debye-Hückel equation, i.e., $\Delta c_i(x, z) - \kappa_i^2 c_i(x, z) = 0$, where $i = 1$ (2) corresponds to $x > 0$ (< 0), (ii) $\partial_z c_i(x, z) = 0$ at $z = \pm L$, (iii) $c_i(x = \pm\infty, z) = 0$, (iv) $c_1(0^+, z) + \Psi_1(z) = c_2(0^-, z) + \Psi_2(z)$, and (v), due to $\partial_x \Psi_i(z) = 0$, $\varepsilon_1 \partial_x c_1(0^+, z) = \varepsilon_2 \partial_x c_2(0^-, z)$. It is clear from the construction that $c_i(x, z)$ keeps all the conditions, which are already satisfied by $\bar{\Phi}_i(x) + \Psi_i(z)$, unchanged and takes care of the continuity of the total potential at the interface. Therefore the exact electrostatic potential (superscript "e") is given by $\Phi_i^e(x, z) = \bar{\Phi}_i(x) + \Psi_i(z) + c_i(x, z)$.

In order to determine the correction function $c_i(x, z)$ we expand its dependence on $z \in [-L, L]$ into a Fourier series:

$$c_i(x, z) = \frac{a_{0,i}(x)}{2} + \sum_{n=1}^{\infty} a_{n,i}(x) \cos\left(\frac{n\pi z}{L}\right) + \sum_{n=1}^{\infty} b_{n,i}(x) \sin\left(\frac{n\pi z}{L}\right).$$

The boundary condition $\partial_z c_i(x, \pm L) = 0$ leads to $b_{n,i}(x) = 0$, so that

$$c_i(x, z) = \frac{a_{0,i}(x)}{2} + \sum_{n=1}^{\infty} a_{n,i}(x) \cos\left(\frac{n\pi z}{L}\right). \tag{A5}$$

Inserting this expression into the Debye-Hückel equation (condition (i) listed above) one obtains

$$\frac{a_{0,i}''(x)}{2} - \kappa_i^2 \frac{a_{0,i}(x)}{2} + \sum_{n=1}^{\infty} a_{n,i}''(x) \cos\left(\frac{n\pi z}{L}\right) - \frac{n^2\pi^2}{L^2} \sum_{n=1}^{\infty} a_{n,i}(x) \cos\left(\frac{n\pi z}{L}\right) - \kappa_i^2 \sum_{n=1}^{\infty} a_{n,i}(x) \cos\left(\frac{n\pi z}{L}\right) = 0,$$

which implies

$$a_{0,i}''(x) - \kappa_i^2 a_{0,i}(x) = 0,$$

$$a_{n,i}''(x) - \left[\left(\frac{n\pi}{L}\right)^2 + \kappa_i^2\right] a_{n,i}(x) = 0.$$

As solutions for these two equations one obtains

$$a_{0,i}(x) = D_i e^{-\kappa_i x} + C_i e^{\kappa_i x},$$
$$a_{n,i}(x) = A_{n,i} e^{-\sqrt{\left(\frac{n\pi}{L}\right)^2+\kappa_i^2}x} + B_{n,i} e^{\sqrt{\left(\frac{n\pi}{L}\right)^2+\kappa_i^2}x}.$$

Due to the boundary condition $c_i(\pm\infty, z) = 0$ the coefficients $a_{0,i}$ and $a_{n,i}$ in the two media are given by

$$a_{0,1}(x) = D_1 e^{-\kappa_1 x},$$
$$a_{n,1}(x) = A_{n,1} e^{-\sqrt{\left(\frac{n\pi}{L}\right)^2+\kappa_1^2}x}, \qquad \text{in medium 1,}$$

and

$$a_{0,2}(x) = C_2 e^{\kappa_2 x},$$
$$a_{n,2}(x) = B_{n,2} e^{\sqrt{\left(\frac{n\pi}{L}\right)^2+\kappa_2^2}x}, \qquad \text{in medium 2.}$$

With this Eq. (A5) can be written as ($D_1 = D,\ C_2 = C,\ A_{n,1} = A_n,$ and $B_{n,2} = B_n$)

$$c_1(x,z) = \frac{De^{-\kappa_1 x}}{2} + \sum_{n=1}^{\infty} A_n e^{-\sqrt{\left(\frac{n\pi}{L}\right)^2+\kappa_1^2}x} \cos\left(\frac{n\pi z}{L}\right), \tag{A6a}$$

$$c_2(x,z) = \frac{Ce^{\kappa_2 x}}{2} + \sum_{n=1}^{\infty} B_n e^{\sqrt{\left(\frac{n\pi}{L}\right)^2+\kappa_2^2}x} \cos\left(\frac{n\pi z}{L}\right). \tag{A6b}$$

In order to determine the constants A_n, B_n, C, and D, the boundary conditions (iv) and (v) are used:

$$\frac{2\sigma_1}{\kappa_1^2\varepsilon_1 L} + D = \frac{2\sigma_2}{\kappa_2^2\varepsilon_2 L} + C, \tag{A7a}$$

$$\frac{2\sigma_1}{\kappa_1^2\varepsilon_1 L}\frac{(-1)^n}{\left(1+\frac{n^2\pi^2}{\kappa_1^2 L^2}\right)} + A_n = \frac{2\sigma_2}{\kappa_2^2\varepsilon_2 L}\frac{(-1)^n}{\left(1+\frac{n^2\pi^2}{\kappa_2^2 L^2}\right)} + B_n, \tag{A7b}$$

$$-\varepsilon_1\kappa_1 D = \varepsilon_2\kappa_2 C, \tag{A7c}$$

$$-\varepsilon_1\sqrt{\left(\frac{n\pi}{L}\right)^2+\kappa_1^2}A_n = \varepsilon_2\sqrt{\left(\frac{n\pi}{L}\right)^2+\kappa_2^2}B_n. \tag{A7d}$$

Here we have used the relationships $\int_{-L}^{L}\cos\left(\frac{n\pi z}{L}\right)\ dz = 0$, $\int_{-L}^{L}\cos\left(\frac{n\pi z}{L}\right)\cos\left(\frac{m\pi z}{L}\right)\ dz = L\delta_{n,m}$, and $\int_{-L}^{L}\cosh(\kappa z)\cos\left(\frac{m\pi z}{L}\right)\ dz = 2\kappa(-1)^m\left[\kappa^2+\left(\frac{m\pi}{L}\right)^2\right]^{-1}\sinh(\kappa L)$ (Eq. (2.671.4) in Ref. [32]). Solving these four equations one finally arrives at the following expressions for

the electrostatic potential in the two media:

$$\Phi_1^e(x,z) = \frac{\sigma_1}{\kappa_1\varepsilon_1}\frac{\cosh\kappa_1 z}{\sinh(\kappa_1 L)} + \frac{\kappa_2\varepsilon_2\Phi_D}{\kappa_1\varepsilon_1+\kappa_2\varepsilon_2}e^{-\kappa_1 x} + \frac{1}{L}\frac{\frac{\sigma_2}{\kappa_2^2\varepsilon_2}-\frac{\sigma_1}{\kappa_1^2\varepsilon_1}}{1+\frac{\kappa_1\varepsilon_1}{\kappa_2\varepsilon_2}}e^{-\kappa_1 x} + 2L\sum_{n=1}^{\infty}(-1)^n\frac{\frac{\sigma_2}{\varepsilon_2}\frac{1}{n^2\pi^2+\kappa_2^2L^2}-\frac{\sigma_1}{\varepsilon_1}\frac{1}{n^2\pi^2+\kappa_1^2L^2}}{1+\frac{\varepsilon_1\sqrt{n^2\pi^2+\kappa_1^2L^2}}{\varepsilon_2\sqrt{n^2\pi^2+\kappa_2^2L^2}}}e^{-\sqrt{\left(\frac{n\pi}{L}\right)^2+\kappa_1^2}x}\cos\left(\frac{n\pi z}{L}\right), \tag{A8}$$

and

$$\Phi_2^e(x,z) = \frac{\sigma_2}{\kappa_2\varepsilon_2}\frac{\cosh(\kappa_2 z)}{\sinh(\kappa_2 L)} + \Phi_D\left(1-\frac{\kappa_1\varepsilon_1}{\kappa_1\varepsilon_1+\kappa_2\varepsilon_2}e^{\kappa_2 x}\right) + \frac{1}{L}\frac{\frac{\sigma_1}{\kappa_1^2\varepsilon_1}-\frac{\sigma_2}{\kappa_2^2\varepsilon_2}}{1+\frac{\kappa_2\varepsilon_2}{\kappa_1\varepsilon_1}}e^{\kappa_2 x} + 2L\sum_{n=1}^{\infty}(-1)^n\frac{\frac{\sigma_1}{\varepsilon_1}\frac{1}{n^2\pi^2+\kappa_1^2L^2}-\frac{\sigma_2}{\varepsilon_2}\frac{1}{n^2\pi^2+\kappa_2^2L^2}}{1+\frac{\varepsilon_2\sqrt{n^2\pi^2+\kappa_2^2L^2}}{\varepsilon_1\sqrt{n^2\pi^2+\kappa_1^2L^2}}}e^{\sqrt{\left(\frac{n\pi}{L}\right)^2+\kappa_2^2}x}\cos\left(\frac{n\pi z}{L}\right). \tag{A9}$$

Equations (A8) and (A9) can be expressed in terms of a single equation:

$$\Phi_i^e(x,z) = \Phi_{bi} + \sum_{j\in\{1,2\}}^{j\neq i}\frac{(-1)^j\kappa_j\varepsilon_j\Phi_D}{\kappa_1\varepsilon_1+\kappa_2\varepsilon_2}e^{-\kappa_i|x|} + \Phi_i^{(0)}\frac{\cosh(\kappa_i z)}{\sinh(\kappa_i L)} + \sum_{j\in\{1,2\}}^{j\neq i}\frac{C_{ij}^{(0)}(L)e^{-a_i^{(0)}(L)|x|}}{2} + \sum_{j\in\{1,2\}}^{j\neq i}\sum_{n=1}^{\infty}C_{ij}^{(n)}(L)e^{-a_i^{(n)}(L)|x|}\cos\left(\frac{n\pi z}{L}\right), \tag{A10}$$

with $\Phi_i^{(0)} = \sigma_i/(\varepsilon_i\kappa_i)$, $a_i^{(n)}(L) = \sqrt{\left(\frac{n\pi}{L}\right)^2+\kappa_i^2}$, $\Phi_{b1}=0$, $\Phi_{b2}=\Phi_D$, and

$$C_{ij}^{(n)}(L) = 2L(-1)^n\frac{\frac{\sigma_j}{\varepsilon_j}\frac{1}{n^2\pi^2+\kappa_j^2L^2}-\frac{\sigma_i}{\varepsilon_i}\frac{1}{n^2\pi^2+\kappa_i^2L^2}}{1+\frac{\varepsilon_i\sqrt{n^2\pi^2+\kappa_i^2L^2}}{\varepsilon_j\sqrt{n^2\pi^2+\kappa_j^2L^2}}}. \tag{A11}$$

Equation (A10) is identical to Eq. (1) with the coefficients $C_{ij}^{(n)}(L)$ given by Eq. (A11).

We have checked that exactly the same result can be obtained by following the procedure adopted by Domínguez *et al.* [21].

2. Superposition approximation

First, we determine the electrostatic potential due to a *single* charged planar wall located at $z=0$ confining a semi-infinite interface between two electrolytes (Fig. 4(a)). Also in this case we divide the problem into three sub-problems (Figs. 4(b)-(d)): (i) a fluid interface only in the absence of any wall, (ii) a homogeneously charged wall with surface charge density

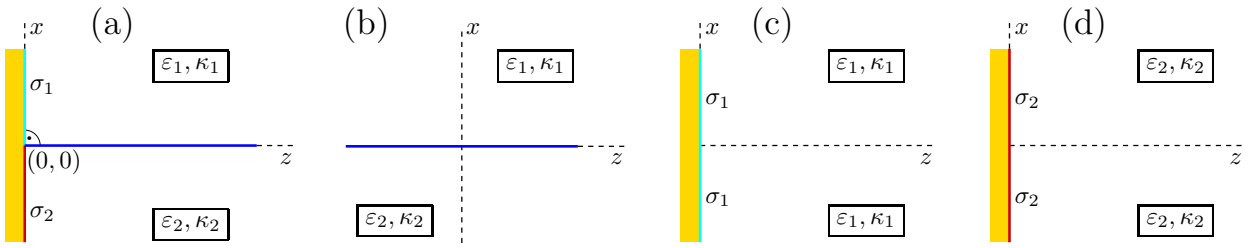

FIG. 4: (a) Sketch of the problem with a *single* planar wall in the presence of a semi-infinite interface formed by electrolyte "1" and "2" with permittivities ε_1 and ε_2 as well as inverse Debye lengths κ_1 and κ_2, respectively. In order to facilitate the calculation of the electrostatic potential the problem is sub-divided into three parts: (i) the electrolytes "1" and "2" separated by an interface at $x = 0$ in the absence of any wall [(b)], (ii) a single homogeneous wall at $z = 0$ carrying a charge density σ_1 bounding a uniform half-space filled by electrolyte "1" [(c)], and (iii) a single homogeneous wall at $z = 0$ carrying a charge density σ_2 bounding a uniform half-space filled by electrolyte "2" [(d)].

σ_1, bounding a half-space filled by uniform medium "1", and (iii) a homogeneously charged wall with surface charge density σ_2 bounding a half-space filled by uniform medium "2". After solving these three sub-problems a correction function is constructed which satisfies the following boundary conditions for the total electrostatic potential: (i) it is finite for $z \to \infty$ or $x \to \pm\infty$, (ii) the electrostatic potential and the normal component of the electric displacement field are continuous at the interface, and (iii) the normal component of the electric displacement field at the wall corresponds to the local surface charge density at the wall.

a. Solution of sub-problem (i)

This part of the problem is identical to the sub-problem (i) we have considered for the exact solution. Thus the potentials in the two media are given by Eq. (A2).

b. Solutions of sub-problems (ii) and (iii)

For a charged wall at $z = 0$ carrying a charge density σ_1 in contact with the uniform electrolyte "1", the electrostatic potential is given by the solution of

$$\Delta\Psi_1(z) - \kappa_1^2\Psi_1(z) = 0,$$

where $\Delta = d^2/dz^2$. The solution to this equation is given by

$$\Psi_1(z) = Ee^{-\kappa_1 z} + Fe^{\kappa_1 z}.$$

The boundary condition $\Psi_1(z \to \infty) \to 0$ leads to $F = 0$. In order to find the integration constant E the boundary condition that the electric displacement field should be equal to the charge density at the wall, i.e., $-\varepsilon_1\partial_z\Psi_1(0) = \sigma_1$ is used. The final expression reads

$$\Psi_1(z) = \frac{\sigma_1}{\kappa_1\varepsilon_1}e^{-\kappa_1 z}. \tag{A12}$$

Sub-problem (iii) can be solved analogously and the solution is given by

$$\Psi_2(z) = \frac{\sigma_2}{\kappa_2\varepsilon_2}e^{-\kappa_2 z}. \tag{A13}$$

c. Construction of the correction function and final solution

We seek a correction function $c_i(x, z)$ such that (i) $c_i(x, z)$ is a solution of the Debye-Hückel equation, i.e., $\Delta c_i(x, z) - \kappa_i^2 c_i(x, z) = 0$ where $i = 1$ (2) corresponds to $x > 0$ (< 0), (ii) $\partial_z c_i(x, z) = 0$ at $z = 0$, (iii) $c_i(x = \pm\infty, z) = c_i(x, z = \infty) = 0$, (iv) $c_1(0^+, z) + \Psi_1(z) = c_2(0^-, z) + \Psi_2(z)$, and (v) $\varepsilon_1\partial_x c_1(0^+, z) = \varepsilon_2\partial_x c_2(0^-, z)$. Accordingly the final solution for the electrostatic potential of a single wall in each medium is given by $\Phi_i(x, z) = \bar{\Phi}_i(x) + \Psi_i(z) + c_i(x, z)$. In order to determine this correction function we extend the system to $z \in [-\infty, \infty]$ and solve the Debye-Hückel equation in the entire space by taking the Fourier transform with respect to z [26]. The second condition listed above is satisfied automatically because the system is symmetric about the plane $z = 0$. If a solution for $z \in \mathbb{R}$ satisfies this boundary condition at $z = 0$, it is the solution looked for in the range $z > 0$. Therefore we are looking for a solution of the equation

$$\left(\partial_x^2 + \partial_z^2 - \kappa_i^2\right) c_i(x, z) = 0, \tag{A14}$$

with

$$c_i(x,z) = \frac{1}{2\pi}\int\limits_{-\infty}^{\infty} dq\ \hat{c}_i(x,q)e^{iqz}, \quad \hat{c}_i(x,q) = \int\limits_{-\infty}^{\infty} dz\ c_i(x,z)e^{-iqz}, \tag{A15}$$

or equivalently

$$\left(\partial_x^2 - q^2 - \kappa_i^2\right)\hat{c}_i(x,q) = 0. \tag{A16}$$

For the two media "1" and "2", the solutions of Eq. (A16) which fulfill boundary condition (iii) can be written as

$$\hat{c}_1(x,q) = M_1(q)e^{-p_1 x}, \qquad p_1 > 0, \tag{A17a}$$

$$\hat{c}_2(x,q) = M_2(q)e^{p_2 x}, \qquad p_2 > 0, \tag{A17b}$$

with $p_i^2 = q^2 + \kappa_i^2$. In order to determine $M_1(q)$ and $M_2(q)$, boundary conditions (iv) and (v) are used. To apply the fourth condition the Fourier transforms $\hat{\Psi}_i(q)$ of $\Psi_i(z) = \frac{\sigma_i}{\kappa_i\varepsilon_i}e^{-\kappa_i|z|}$ (in line with the above symmetry argument, Eqs. (A12) and (A13)) are needed:

$$\hat{\Psi}_1(q) = \frac{\sigma_1}{\kappa_1\varepsilon_1}\frac{2\kappa_1}{q^2+\kappa_1^2} = B_1\frac{2\kappa_1}{q^2+\kappa_1^2},$$
$$\hat{\Psi}_2(q) = \frac{\sigma_2}{\kappa_2\varepsilon_2}\frac{2\kappa_2}{q^2+\kappa_2^2} = B_2\frac{2\kappa_2}{q^2+\kappa_2^2},$$

where $B_i = \sigma_i/(\kappa_i\varepsilon_i)$. Using these, boundary conditions (iv) and (v) lead to the following set of equations

$$\frac{2\kappa_1 B_1}{q^2+\kappa_1^2} + M_1(q) = \frac{2\kappa_2 B_2}{q^2+\kappa_2^2} + M_2(q),$$
$$-\varepsilon_1 p_1 M_1(q) = \varepsilon_2 p_2 M_2(q).$$

Solving this set of equations for $M_1(q)$ and $M_2(q)$ and inserting into Eqs. (A17a) and (A17b) leads to the following expressions:

$$c_1(x,z) = \frac{1}{\pi}\int_{-\infty}^{\infty} dq\ \frac{\varepsilon_2 p_2}{\varepsilon_1 p_1 + \varepsilon_2 p_2}\left(\frac{-\kappa_1 B_1}{q^2+\kappa_1^2} + \frac{\kappa_2 B_2}{q^2+\kappa_2^2}\right)e^{-p_1 x + iqz}, \tag{A18a}$$

$$c_2(x,z) = -\frac{1}{\pi}\int_{-\infty}^{\infty} dq\ \frac{\varepsilon_1 p_1}{\varepsilon_1 p_1 + \varepsilon_2 p_2}\left(\frac{-\kappa_1 B_1}{q^2+\kappa_1^2} + \frac{\kappa_2 B_2}{q^2+\kappa_2^2}\right)e^{p_2 x + iqz}. \tag{A18b}$$

Since apart from the factor $\exp(iqz)$ both integrands are even functions of q, one finds that indeed boundary condition (ii), i.e., $\partial_z c_i(x,z) = 0$ for $z = 0$ is fulfilled. Moreover, this symmetry allows one to write these expressions in terms of trigonometric functions so that

one arrives at the following final expressions for the electrostatic potentials in the two media:

$$\Phi_1(x,z) = \frac{\sigma_1}{\kappa_1\varepsilon_1}e^{-\kappa_1 z} + \frac{\kappa_2\varepsilon_2\Phi_D}{\kappa_1\varepsilon_1+\kappa_2\varepsilon_2}e^{-\kappa_1 x} + \frac{2\varepsilon_2}{\pi}\int_0^\infty dq \frac{\sqrt{q^2+\kappa_2^2}\cos(qz)e^{-\sqrt{q^2+\kappa_1^2}x}}{\varepsilon_1\sqrt{q^2+\kappa_1^2}+\varepsilon_2\sqrt{q^2+\kappa_2^2}}\left(\frac{-\sigma_1}{\varepsilon_1(q^2+\kappa_1^2)}+\frac{\sigma_2}{\varepsilon_2(q^2+\kappa_2^2)}\right), \quad \text{(A19)}$$

and

$$\Phi_2(x,z) = \frac{\sigma_2}{\kappa_2\varepsilon_2}e^{-\kappa_2 z} + \Phi_D\left(1-\frac{\kappa_1\varepsilon_1}{\kappa_1\varepsilon_1+\kappa_2\varepsilon_2}e^{\kappa_2 x}\right) + \frac{2\varepsilon_1}{\pi}\int_0^\infty dq \frac{\sqrt{q^2+\kappa_1^2}\cos(qz)e^{\sqrt{q^2+\kappa_2^2}x}}{\varepsilon_1\sqrt{q^2+\kappa_1^2}+\varepsilon_2\sqrt{q^2+\kappa_2^2}}\left(\frac{\sigma_1}{\varepsilon_1(q^2+\kappa_1^2)}-\frac{\sigma_2}{\varepsilon_2(q^2+\kappa_2^2)}\right). \quad \text{(A20)}$$

Equations (A19) and (A20) express the electrostatic potential in the two media due to a single charged plane located at $z = 0$. The superposition approximation amounts to approximate the electrostatic potential between two charged walls at $z = \pm L$ by the sum of the electrostatic potentials due to two identical charged walls at $z = -L$ and $z = +L$. This is accomplished via shifting the potential Φ_i by $-L$ to left, by $+L$ to the right, reflecting the latter about its new position, and adding the former and the latter (the superscript "s" indicates the solution obtained within the superposition approximation): $\Phi_i^s(x,z) = \Phi_i(x,z+L) + \Phi_i(x,-(z-L))$ so that

$$\Phi_1^s(x,z) = \frac{2\sigma_1}{\kappa_1\varepsilon_1}e^{-\kappa_1 L}\cosh(\kappa_1 z) + \frac{2\kappa_2\varepsilon_2\Phi_D}{\kappa_1\varepsilon_1+\kappa_2\varepsilon_2}e^{-\kappa_1 x} + \frac{4\varepsilon_2}{\pi}\int_0^\infty dq\ \frac{\sqrt{q^2+\kappa_2^2}\cos(qL)\cos(qz)}{\varepsilon_1\sqrt{q^2+\kappa_1^2}+\varepsilon_2\sqrt{q^2+\kappa_2^2}}\left(\frac{-\sigma_1}{\varepsilon_1(q^2+\kappa_1^2)}+\frac{\sigma_2}{\varepsilon_2(q^2+\kappa_2^2)}\right)e^{-\sqrt{q^2+\kappa_1^2}x} \quad \text{(A21)}$$

and

$$\Phi_2^s(x,z) = \frac{2\sigma_2}{\kappa_2\varepsilon_2}e^{-\kappa_2 L}\cosh(\kappa_2 z) + 2\Phi_D\left(1-\frac{\kappa_1\varepsilon_1}{\kappa_1\varepsilon_1+\kappa_2\varepsilon_2}e^{\kappa_2 x}\right) + \frac{4\varepsilon_1}{\pi}\int_0^\infty dq\ \frac{\sqrt{q^2+\kappa_1^2}\cos(qL)\cos(qz)}{\varepsilon_1\sqrt{q^2+\kappa_1^2}+\varepsilon_2\sqrt{q^2+\kappa_2^2}}\left(\frac{\sigma_1}{\varepsilon_1(q^2+\kappa_1^2)}-\frac{\sigma_2}{\varepsilon_2(q^2+\kappa_2^2)}\right)e^{\sqrt{q^2+\kappa_2^2}x}. \quad \text{(A22)}$$

Equations (A21) and (A22) can be expressed by a single equation of the form

$$\Phi_i^s(x,z) = 2\Phi_{bi} + \sum_{j\in\{1,2\}}^{j\neq i}\frac{2(-1)^j\kappa_j\varepsilon_j\Phi_D}{\kappa_1\varepsilon_1+\kappa_2\varepsilon_2}e^{-\kappa_i|x|} + 2\Phi_i^{(0)}\cosh(\kappa_i z)e^{-\kappa_i L} + \sum_{j\in\{1,2\}}^{j\neq i}\int_0^\infty dq\ C_{ij}^s(q)\cos(qL)\cos(qz)e^{-\sqrt{q^2+\kappa_i^2}|x|} \quad \text{(A23)}$$

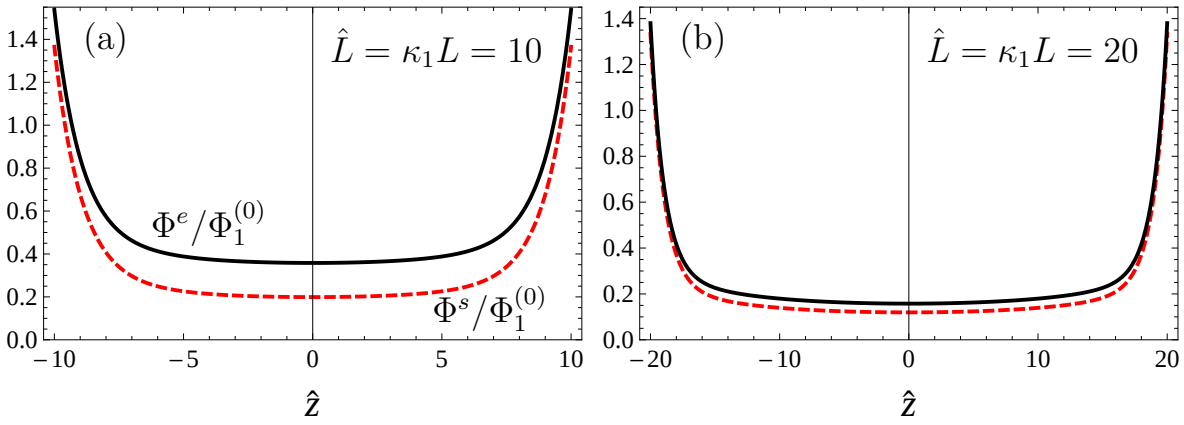

FIG. 5: Comparison between the exact expression (superscript "e", black solid lines, see Eq. (1)) and the superposition approximation (superscript "s", red dashed lines, see Eq. (2)) of the electrostatic potential $\Phi(x,z)$ at the interfacial plane ($x=0$) in units of $\Phi_1^{(0)} = \sigma_1/(\kappa_1\varepsilon_1)$ for varying $\hat{z} = \kappa_1 z$ and two slit widths: $\hat{L} = \kappa_1 L = 10$ (panel (a)) and $\hat{L} = \kappa_1 L = 20$ (panel (b)). For the plots typical parameter ratios $\kappa = \kappa_2/\kappa_1 = 0.025$, $\varepsilon = \varepsilon_2/\varepsilon_1 = 0.025$, $\sigma = \sigma_2/\sigma_1 = 0.1$, and $\Phi_D/\Phi_1^{(0)} = 1.3$ have been chosen. Φ^e and Φ^s differ significantly at narrow widths L, and the difference between the two expressions decreases upon increasing the slit width. In the limit $\hat{z} \to \pm\hat{L}$, both Φ^e and Φ^s remain finite.

with $\Phi_i^{(0)} = \sigma_i/(\varepsilon_i\kappa_i)$, $\Phi_{b1} = 0$, $\Phi_{b2} = \Phi_D$, and

$$C_{ij}^s(q) = \frac{4\varepsilon_j}{\pi} \frac{\sqrt{q^2+\kappa_j^2}}{\varepsilon_i\sqrt{q^2+\kappa_i^2} + \varepsilon_j\sqrt{q^2+\kappa_j^2}} \left(\frac{\sigma_j}{\varepsilon_j(q^2+\kappa_j^2)} - \frac{\sigma_i}{\varepsilon_i(q^2+\kappa_i^2)} \right). \tag{A24}$$

Equation (A23) corresponds to (Eq. (2)) with the coefficients $C_{ij}^s(q)$ given by Eq. (A24).

A comparison between the exact and the approximate potential is given in Fig. 5.

Appendix B: Grand potential

1. Density functional

The model we are considering corresponds to the grand canonical density functional

$$\beta\Omega\left[\varrho_\pm\right] = \int_V d^3r \left[\sum_{i=\pm} \varrho_i(\mathbf{r}) \left\{ \ln\left(\frac{\varrho_i(\mathbf{r})}{\zeta_i} \right) - 1 + \beta V_i(\mathbf{r}) \right\} + \frac{\beta \mathbf{D}\left(\mathbf{r}, [\varrho_\pm]\right)^2}{2\varepsilon(\mathbf{r})} \right], \tag{B1}$$

where '+' and '−' indicate the positive and negative ions respectively, $\beta = 1/(k_B T)$ is the inverse thermal energy, $\varrho_\pm(\mathbf{r})$ are the number densities of the ionic components, $\zeta_\pm$ represent the fugacities of the two ion-species, and $\varepsilon(\mathbf{r})$ denotes the permittivity with $\varepsilon(\mathbf{r}) = \varepsilon_1$ (ε_2) for $x > 0$ ($x < 0$). Since the salt reservoir is provided by the bulk of media '1' and '2', we use the freedom to shift the potentials $V_\pm(\mathbf{r})$, which describe the ion-solvent interactions due to solvation, such that $V_\pm(\mathbf{r}) = 0$ in medium '1' ($x > 0$) and $V_\pm(\mathbf{r}) = f_\pm$ in medium '2' ($x < 0$). Hence $f_\pm$ correspond to the ion solvation free energy differences between media '2' and '1'. The integration volume V is the slab formed in between the two charged planar walls. According to Gauss' law $\nabla \cdot \mathbf{D}(\mathbf{r}, [\varrho_\pm]) = \sum_{i=\pm} e q_i \varrho_i(\mathbf{r})$ with $e > 0$ the elementary charge and $q_\pm = \pm 1$. We consider Neumann-type boundary conditions at the walls, i.e., $\mathbf{n}(\mathbf{r}) \cdot \mathbf{D}(\mathbf{r}, [\varrho_\pm]) = -\sigma(\mathbf{r})$ with the electric displacement field $\mathbf{D}$ and the charge density at the walls $\sigma(\mathbf{r})$. In Eq. (B1) the sum represents the entropic ideal gas contribution of the ions and the last term represents the energy contribution due to the electrostatic Coulomb interaction between the ions which is expressed in terms of the electrostatic energy density [33]. In this model the ions are pointlike particles.

2. Expansion of the density functional

Denoting the deviations of the ion number densities from the bulk ionic strength $I(\mathbf{r})$ ($I(\mathbf{r}) = I_1$ for $x > 0$ and $I(\mathbf{r}) = I_2$ for $x < 0$) by $\phi_\pm(\mathbf{r}) := \varrho_\pm(\mathbf{r}) - I(\mathbf{r})$ and expanding the grand potential functional $\beta\Omega[\varrho_\pm]$ in terms of the small deviations ϕ_i up to quadratic order one obtains

$$\begin{aligned}\beta\Omega[\varrho_\pm] = &\int_V d^3r \sum_{i=\pm} I(\mathbf{r}) \left[\ln\left(\frac{I(\mathbf{r})}{\zeta_i}\right) - 1 + \beta V_i(\mathbf{r})\right] \\ &+ \int_V d^3r \left[\sum_{i=\pm} \phi_i(\mathbf{r}) \left\{\ln\left(\frac{I(\mathbf{r})}{\zeta_i}\right) + \beta V_i(\mathbf{r}) + \frac{\phi_i(\mathbf{r})}{2I(\mathbf{r})}\right\} + \frac{\beta \mathbf{D}(\mathbf{r}, [\varrho_\pm])^2}{2\varepsilon(\mathbf{r})}\right] + \mathcal{O}(\phi^3).\end{aligned}$$

Here the first line ($\mathcal{O}(\phi^0)$) describes the bulk contribution and the integrals in the second line ($\mathcal{O}(\phi^n); n \geq 1$) represent the surface and line contributions to the free energy (note that $\mathbf{D} = \mathcal{O}(\phi)$, see below). For future convenience we denote the latter by $\beta\mathcal{H}[\phi_\pm]$:

$$\beta\mathcal{H}[\phi_\pm] = \int_V d^3r \left[\sum_{i=\pm} \phi_i(\mathbf{r}) \left\{\ln\left(\frac{I(\mathbf{r})}{\zeta_i}\right) + \beta V_i(\mathbf{r}) + \frac{\phi_i(\mathbf{r})}{2I(\mathbf{r})}\right\} + \frac{\beta \mathbf{D}(\mathbf{r}, [\phi_\pm])^2}{2\varepsilon(\mathbf{r})}\right]. \qquad \text{(B2)}$$

3. Minimization of the density functional

Minimization of $\beta\mathcal{H}\left[\phi_{\pm}\right]$ leads to the Euler-Lagrange equation $\delta\left(\beta\mathcal{H}\left[\phi_{\pm}\right]\right)=0$. Equation (B2) implies

$$\delta\left(\beta\mathcal{H}\left[\phi_{\pm}\right]\right)=\int_{V}d^{3}r\ \left[\sum_{i=\pm}\delta\phi_{i}(\mathbf{r})\left\{\ln\left(\frac{I(\mathbf{r})}{\zeta_{i}}\right)+\beta V_{i}(\mathbf{r})+\frac{\phi_{i}(\mathbf{r})}{I(\mathbf{r})}\right\}\right] + \int_{V}d^{3}r\ \frac{\beta\mathbf{D}\left(\mathbf{r},\left[\phi_{\pm}\right]\right)}{\varepsilon(\mathbf{r})}\cdot\delta\mathbf{D}\left(\mathbf{r},\left[\phi_{\pm}\right]\right). \tag{B3}$$

Using the relation $\mathbf{D}\left(\mathbf{r},\left[\phi_{\pm}\right]\right)=-\varepsilon(\mathbf{r})\nabla\Phi\left(\mathbf{r},\left[\phi_{\pm}\right]\right)$, with $\Phi\left(\mathbf{r},\left[\phi_{\pm}\right]\right)$ denoting the electrostatic potential, and the divergence theorem, the last term in Eq. (B3) can be written as

$$\begin{aligned}&\int_{V}d^{3}r\ \frac{\beta\mathbf{D}\left(\mathbf{r},\left[\phi_{\pm}\right]\right)}{\varepsilon(\mathbf{r})}\cdot\delta\mathbf{D}\left(\mathbf{r},\left[\phi_{\pm}\right]\right)\\&=\int_{V}d^{3}r\ \beta\left(-\nabla\Phi\left(\mathbf{r},\left[\phi_{\pm}\right]\right)\right)\cdot\delta\mathbf{D}\left(\mathbf{r},\left[\phi_{\pm}\right]\right)\\&=-\beta\int_{\partial V}d^{2}r\ \Phi\left(\mathbf{r},\left[\phi_{\pm}\right]\right)\mathbf{n}(\mathbf{r})\cdot\delta\mathbf{D}\left(\mathbf{r},\left[\phi_{\pm}\right]\right)+\beta\int_{V}d^{3}r\ \Phi\left(\mathbf{r},\left[\phi_{\pm}\right]\right)\delta\nabla\cdot\mathbf{D}\left(\mathbf{r},\left[\phi_{\pm}\right]\right).\end{aligned}$$

The Neumann boundary condition leads to $\mathbf{n}(\mathbf{r})\cdot\delta\mathbf{D}\left(\mathbf{r},\left[\phi_{\pm}\right]\right)=-\delta\sigma(\mathbf{r})=0$. According to electrostatics one has $\nabla\cdot\mathbf{D}\left(\mathbf{r},\left[\phi_{\pm}\right]\right)=\sum\limits_{i=\pm}eq_{i}\varrho_{i}(\mathbf{r})=\sum\limits_{i=\pm}eq_{i}\left(\phi_{i}(\mathbf{r})+I(\mathbf{r})\right)=\sum\limits_{i=\pm}eq_{i}\phi_{i}(\mathbf{r})$ (as $\sum\limits_{i=\pm}q_{i}I(\mathbf{r})=0$). This implies

$$\delta\left(\beta\mathcal{H}\left[\phi_{\pm}\right]\right)=\int_{V}d^{3}r\ \sum_{i=\pm}\delta\phi_{i}(\mathbf{r})\left[\ln\left(\frac{I(\mathbf{r})}{\zeta_{i}}\right)+\beta V_{i}(\mathbf{r})+\frac{\phi_{i}(\mathbf{r})}{I(\mathbf{r})}+\beta eq_{i}\Phi\left(\mathbf{r},\left[\phi_{\pm}\right]\right)\right]. \tag{B4}$$

The Euler-Lagrange equation leads to

$$\ln\left(\frac{I(\mathbf{r})}{\zeta_{i}}\right)+\beta V_{i}(\mathbf{r})+\frac{\phi_{i}(\mathbf{r})}{I(\mathbf{r})}+\beta eq_{i}\Phi\left(\mathbf{r},\left[\phi_{\pm}\right]\right)=0. \tag{B5}$$

We first discuss the bulk phases.

a. Bulk of phase 1 ($x>0$)

In the bulk of phase 1 one has $I(\mathbf{r})=I_{1}$, $\beta V_{\pm}(\mathbf{r})=0$, $\phi_{\pm}(\mathbf{r})=0$, and $\Phi\left(\mathbf{r},\left[\phi_{\pm}\right]\right)=0$. Therefore Eq. (B5) gives

$$\ln\left(\frac{I_{1}}{\zeta_{\pm}}\right)=0 \tag{B6}$$

so that

$$\zeta_{\pm} = I_1. \tag{B7}$$

b. Bulk of phase 2 ($x < 0$)

In the bulk of phase 2 one has $I(\mathbf{r}) = I_2$, $\beta V_{\pm}(\mathbf{r}) = \beta f_{\pm}$, $\phi_{\pm}(\mathbf{r}) = 0$, and $\Phi(\mathbf{r}, [\phi_{\pm}]) = \Phi_D$, where Φ_D is the Donnan potential (Galvani potential difference). Accordingly, Eq. (B5) gives

$$\ln\left(\frac{I_2}{\zeta_{\pm}}\right) + \beta f_{\pm} \pm \beta e \Phi_D = 0. \tag{B8}$$

Using Eq. (B7) this can be written as

$$\ln\left(\frac{I_2}{I_1}\right) + \beta f_{\pm} \pm \beta e \Phi_D = 0. \tag{B9}$$

Adding the two equations in Eq. (B9), one obtains for the partition ratio

$$2\ln\left(\frac{I_2}{I_1}\right) + \beta\left(f_+ + f_-\right) = 0 \tag{B10}$$

so that

$$\frac{I_2}{I_1} = \exp\left(-\frac{\beta}{2}\left(f_+ + f_-\right)\right). \tag{B11}$$

Subtracting the two equations in Eq. (B9) leads to the Donnan potential:

$$\beta\left(f_+ - f_-\right) + 2\beta e \Phi_D = 0 \tag{B12}$$

so that

$$\Phi_D = -\frac{1}{2e}\left(f_+ - f_-\right). \tag{B13}$$

Combining Eqs. (B6) and Eq. (B8) one can write:

$$\ln\left(\frac{I(\mathbf{r})}{\zeta_{\pm}}\right) + \beta V_{\pm}(\mathbf{r}) \pm \beta e \varphi(\mathbf{r}) = 0 \tag{B14}$$

with $\varphi(\mathbf{r})$ introduced such that $\varphi(\mathbf{r}) = 0$ for $x > 0$ and $\varphi(\mathbf{r}) = \Phi_D$ for $x < 0$. Subtracting this bulk contribution from Eq. (B5) one obtains

$$\frac{\phi_i(\mathbf{r})}{I(\mathbf{r})} + \beta e q_i \left(\Phi(\mathbf{r}, [\phi_{\pm}]) - \varphi(\mathbf{r})\right) = 0 \tag{B15}$$

which can be rewritten as

$$\phi_i(\mathbf{r}) = -\beta e q_i I(\mathbf{r}) \left(\Phi\left(\mathbf{r}, [\phi_\pm]\right) - \varphi(\mathbf{r})\right). \tag{B16}$$

With this Gauss' law gives

$$\begin{aligned} -\nabla \cdot \left(\varepsilon(\mathbf{r}) \nabla \Phi\left(\mathbf{r}, [\phi_\pm]\right)\right) &= e \sum_{i=\pm} q_i \phi_i(\mathbf{r}) \\ &= -2\beta e^2 I(\mathbf{r}) \left(\Phi\left(\mathbf{r}, [\phi_\pm]\right) - \varphi(\mathbf{r})\right), \end{aligned} \tag{B17}$$

The permittivity varies steplike as $\varepsilon(\mathbf{r}) = \varepsilon_1 \Theta(x) + \varepsilon_2 \Theta(-x)$ where Θ is the Heaviside step function. Using this Eq. (B17) can be written as

$$\varepsilon_1 \delta(x) \partial_x \Phi(\mathbf{r}, [\phi_\pm]) - \varepsilon_2 \delta(x) \partial_x \Phi(\mathbf{r}, [\phi_\pm]) + \varepsilon(\mathbf{r}) \nabla^2 \Phi\left(\mathbf{r}, [\phi_\pm]\right) = 2\beta e^2 I(\mathbf{r}) \left(\Phi\left(\mathbf{r}, [\phi_\pm]\right) - \varphi(\mathbf{r})\right). \tag{B18}$$

For $x \neq 0$ Eq. (B18) leads to

$$\nabla^2 \left(\Phi\left(\mathbf{r}, [\phi_\pm]\right) - \varphi(\mathbf{r})\right) = \frac{2\beta e^2 I(\mathbf{r})}{\varepsilon(\mathbf{r})} \left(\Phi\left(\mathbf{r}, [\phi_\pm]\right) - \varphi(\mathbf{r})\right), \tag{B19}$$

which is the linearized Poisson-Boltzmann equation

$$\nabla^2 \left(\Phi\left(\mathbf{r}, [\phi_\pm]\right) - \varphi(\mathbf{r})\right) = \kappa(\mathbf{r})^2 \left(\Phi\left(\mathbf{r}, [\phi_\pm]\right) - \varphi(\mathbf{r})\right) \tag{B20}$$

with $\kappa(\mathbf{r})^2 = 2\beta e^2 I(\mathbf{r})/\varepsilon(\mathbf{r})$. Integrating Eq. (B18) with respect to x over the range $[-\alpha, \alpha]$ and taking $\alpha \to 0$ leads to the boundary condition of continuity of the electric displacement field at the interface: $\left(\varepsilon_1 \partial_x \Phi(\mathbf{r}) - \varepsilon_2 \partial_x \Phi(\mathbf{r})\right)|_{x=0} = 0$.

4. Interaction potential

The surface and line contributions to the free energy functional are given by Eq. (B2). Replacing therein $\left(\ln\left(I(\mathbf{r})/\zeta_i\right) + \beta V_i(\mathbf{r})\right)$ by $-\beta e q_i \varphi(\mathbf{r})$ according to Eq. (B14), $\phi_i(\mathbf{r})/(2I(\mathbf{r}))$ by $-\frac{\beta e q_i}{2}\left(\Phi\left(\mathbf{r}, [\phi_\pm]\right) - \varphi(\mathbf{r})\right)$ according to Eq. (B16) and using $\mathbf{D}(\mathbf{r}, [\phi_\pm]) = -\varepsilon(\mathbf{r}) \nabla \Phi(\mathbf{r}, [\phi_\pm])$ with $\nabla \cdot \mathbf{D}\left(\mathbf{r}, [\phi_\pm]\right) = \sum_{i=\pm} e q_i \phi_i(\mathbf{r})$ one can rewrite Eq. (B2) as:

$$\beta \mathcal{H}\left[\phi_\pm\right] = \int_V d^3 r \ \left[-\frac{\beta}{2} \left(\nabla \cdot \mathbf{D}\left(\mathbf{r}, [\phi_\pm]\right)\right) \left(\Phi\left(\mathbf{r}, [\phi_\pm]\right) + \varphi(\mathbf{r})\right) - \frac{\beta}{2} \mathbf{D}\left(\mathbf{r}, [\phi_\pm]\right) \cdot \nabla \Phi\left(\mathbf{r}, [\phi_\pm]\right)\right]. \tag{B21}$$

Using the product rule $\nabla \cdot (f\mathbf{F}) = \nabla f \cdot \mathbf{F} + f \nabla \cdot \mathbf{F}$, where f is a scalar and $\mathbf{F}$ is a vector, this can further be reduced to

$$\mathcal{H}\left[\phi_{\pm}\right] = -\frac{1}{2} \int\limits_{V} d^3r \, \left[\nabla \cdot \left\{\Phi\left(\mathbf{r}, [\phi_{\pm}]\right) \mathbf{D}\left(\mathbf{r}, [\phi_{\pm}]\right)\right\} + \nabla \cdot \left\{\varphi(\mathbf{r}) \mathbf{D}\left(\mathbf{r}, [\phi_{\pm}]\right)\right\} \right.$$
$$\left. - \mathbf{D}\left(\mathbf{r}, [\phi_{\pm}]\right) \cdot \nabla \varphi(\mathbf{r})\right]. \tag{B22}$$

Converting the volume integral into a surface integral by applying the divergence theorem and using the fact that $\nabla \varphi(\mathbf{r}) = -\Phi_D \delta(x) \mathbf{e_x}$, one obtains

$$\mathcal{H}\left[\phi_{\pm}\right] = -\frac{1}{2} \int\limits_{\partial V} d^2r \; \mathbf{n}(\mathbf{r}) \cdot \mathbf{D}\left(\mathbf{r}, [\phi_{\pm}]\right) \left(\Phi\left(\mathbf{r}, [\phi_{\pm}]\right) + \varphi(\mathbf{r})\right) - \frac{\Phi_D}{2} \int\limits_{x=0} d^2r \; D_x\left(\mathbf{r}, [\phi_{\pm}]\right), \tag{B23}$$

where D_x is the x component of the electric displacement field $\mathbf{D}\left(\mathbf{r}, [\phi_{\pm}]\right)$ and $x = 0$ denotes the integration over the interfacial plane. Using the relation $\mathbf{n}(\mathbf{r}) \cdot \mathbf{D}\left(\mathbf{r}, [\phi_{\pm}]\right) = -\sigma(\mathbf{r})$ one finally arrives at the expression

$$\mathcal{H}\left[\phi_{\pm}\right] = \frac{1}{2} \int\limits_{\partial V} d^2r \; \sigma(\mathbf{r}) \left(\Phi\left(\mathbf{r}, [\phi_{\pm}]\right) + \varphi(\mathbf{r})\right) - \frac{\Phi_D}{2} \int\limits_{x=0} d^2r \; D_x\left(\mathbf{r}, [\phi_{\pm}]\right). \tag{B24}$$

If the slab in between the charged planar walls is given by $V = [-L_x, L_x] \times [0, L_y] \times [-L, L]$ Eq. (B24) can be written in the following way (for brevity we skip the explicit functional dependence on $\phi_{\pm}$):

$$\begin{aligned}
\mathcal{H} &= \frac{1}{2} \int\limits_{\partial V} d^2r \; \sigma(\mathbf{r}) \left(\Phi(\mathbf{r}) + \varphi(\mathbf{r})\right) - \frac{\Phi_D}{2} \int\limits_{x=0} d^2r \; D_x(\mathbf{r}) \\
&= \frac{L_y}{2} \int\limits_{-L_x}^{L_x} dx \;\; \left[\sigma(L)(\Phi(x, L) + \varphi(x)) + \sigma(-L)(\Phi(x, -L) + \varphi(x))\right] - \frac{\Phi_D}{2} \int\limits_{x=0} d^2r \; D_x(\mathbf{r}) \\
&= \frac{L_y}{2} \int\limits_{-L_x}^{0} dx \left[\sigma_2(L)(\Phi_2(x, L) + \Phi_D) + \sigma_2(-L)(\Phi_2(x, -L) + \Phi_D)\right] \\
&\quad + \frac{L_y}{2} \int\limits_{0}^{L_x} dx \left[\sigma_1(L)\Phi_1(x, L) + \sigma_1(x, -L)\Phi_1(-L)\right] + \frac{\Phi_D L_y \varepsilon_1}{2} \int\limits_{-L}^{L} dz \; \left[\partial_x \Phi_1(x = 0, z)\right],
\end{aligned}$$

where we have used $D_x(\mathbf{r}) = -\varepsilon_1 \partial_x \Phi_1(x = 0, z)$, exploiting the continuity of the electric displacement field: $\varepsilon_1 \partial_x \Phi_1(x = 0, z) = \varepsilon_2 \partial_x \Phi_2(x = 0, z)$. For our system $\sigma_1(L) = \sigma_1(-L) = \sigma_1$, $\sigma_2(L) = \sigma_2(-L) = \sigma_2$, and the potentials in the two media are also symmetric with

respect to the z-axis, i.e., $\Phi_1(L) = \Phi_1(-L) = \Phi_1$ and $\Phi_2(L) = \Phi_2(-L) = \Phi_2$. Accordingly, one can write

$$\mathcal{H} = L_y\sigma_2 \int_{-L_x}^{0} dx\ \Phi_2(x,L) + L_y\sigma_1 \int_{0}^{L_x} dx\ \Phi_1(x,L) + \frac{\Phi_D L_y \varepsilon_1}{2} \int_{-L}^{L} dz\ [\partial_x \Phi_1(x=0,z)] + L_x L_y \sigma_2 \Phi_D. \quad \text{(B25)}$$

Inserting the expressions for the electrostatic potentials $\Phi_1(x,z)$ and $\Phi_2(x,z)$ given by Eqs. (1) and (2) one can determine the interaction potential from Eq. (B25). It consists of five contributions: (i) the surface tensions acting between the charged walls and the adjacent fluids in contact (times their area of contact), (ii) the interfacial tension acting between the two fluids in contact at the plane $x = 0$ (times the interfacial area), (iii) the line tension at the three-phase contact lines at both walls (times the total length of the three-phase contact lines), (iv) surface interaction energy densities ($\omega_{\gamma,i}(L)$) due to the effective interaction between the two charged walls (times the total surface area of the walls in contact with media $i \in 1,2$), and (v) a line interaction energy density ($\omega_\tau(L)$) due to the effective interaction between the two three-phase contact lines (times the total length of the three-phase contact lines). The first three contributions are independent of the distance $2L$ between the two walls (note that although the interfacial tension is L-independent it is multiplied by the interfacial area which is proportional to L) whereas the last two contributions are L-dependent (expressed by $\Delta\Omega(L)$ in Eq. (3)). After identifying and separating all these terms, one arrives at the expressions for the surface interaction energy densities, given by Eqs. (4) and (5), and for the line interaction energy densities, given by Eqs. (C1) and (C2) below.

Appendix C: Line interaction potential

The exact expression for the line interaction potential (see Eq. (3)) is given by

$$\begin{aligned}\frac{\omega_\tau^e}{\omega_\tau^{(0)}} &= \frac{1}{2\hat{L}}\frac{\frac{2\sigma}{\kappa}-\kappa\varepsilon-\frac{\sigma^2}{\kappa^3\varepsilon}}{1+\kappa\varepsilon} \\ &+ \frac{1}{\hat{L}}\sum_{n=1}^{\infty}\left[\frac{\frac{\sigma}{\varepsilon}\frac{1}{\frac{n^2\pi^2}{\hat{L}^2}+\kappa^2}-\frac{1}{\frac{n^2\pi^2}{\hat{L}^2}+1}}{1+\frac{\sqrt{\frac{n^2\pi^2}{\hat{L}^2}+1}}{\varepsilon\sqrt{\frac{n^2\pi^2}{\hat{L}^2}+\kappa^2}}}\frac{1}{\sqrt{\frac{n^2\pi^2}{\hat{L}^2}+1}}+\frac{\frac{\sigma}{\frac{n^2\pi^2}{\hat{L}^2}+1}-\frac{\sigma^2}{\varepsilon}\frac{1}{\frac{n^2\pi^2}{\hat{L}^2}+\kappa^2}}{1+\frac{\varepsilon\sqrt{\frac{n^2\pi^2}{\hat{L}^2}+\kappa^2}}{\sqrt{\frac{n^2\pi^2}{\hat{L}^2}+1}}}\frac{1}{\sqrt{\frac{n^2\pi^2}{\hat{L}^2}+\kappa^2}}\right] \\ &- \int_0^\infty dx\ \left[\frac{\frac{\sigma}{\varepsilon}\frac{1}{x^2\pi^2+\kappa^2}-\frac{1}{x^2\pi^2+1}}{1+\frac{\sqrt{x^2\pi^2+1}}{\varepsilon\sqrt{x^2\pi^2+\kappa^2}}}\frac{1}{\sqrt{x^2\pi^2+1}}+\frac{\frac{\sigma}{x^2\pi^2+1}-\frac{\sigma^2}{\varepsilon}\frac{1}{x^2\pi^2+\kappa^2}}{1+\frac{\varepsilon\sqrt{x^2\pi^2+\kappa^2}}{\sqrt{x^2\pi^2+1}}}\frac{1}{\sqrt{x^2\pi^2+\kappa^2}}\right] \end{aligned} \tag{C1}$$

with $\omega_\tau^{(0)} = \sigma_1^2/(\kappa_1^2\varepsilon_1)$, $\hat{L} = \kappa_1 L$, $\sigma = \sigma_2/\sigma_1$, $\kappa = \kappa_2/\kappa_1$, and $\varepsilon = \varepsilon_2/\varepsilon_1$. The difference between the infinite sum and the integral is such that in leading order for $\hat{L} \to \infty$ it cancels the first term $\sim 1/\hat{L}$. Also the higher order terms in $(1/\hat{L})$ vanish so that ω_τ^e decays exponentially for large $\hat{L}$. In the opposite limit, i.e., for $\hat{L} \to 0$, ω_τ^e diverges $\sim 1/\hat{L}$.

Within the superposition approximation the line interaction potential is given by

$$\begin{aligned}\frac{\omega_\tau^s}{\omega_\tau^{(0)}} &= \frac{\kappa}{1+\varepsilon\kappa}\left(\frac{\sigma}{\kappa^2}-\varepsilon\right)\frac{\Phi_D}{2\Phi_1^{(0)}} \\ &- \frac{1}{\pi}\frac{\Phi_D}{\Phi_1^{(0)}}\int_0^\infty d\hat{q}\ \frac{\sqrt{\hat{q}^2+1}\sqrt{\hat{q}^2+\kappa^2}}{\sqrt{\hat{q}^2+1}+\varepsilon\sqrt{\hat{q}^2+\kappa^2}}\left[\frac{\sigma}{\hat{q}^2+\kappa^2}-\frac{\varepsilon}{\hat{q}^2+1}\right]\frac{\sin(2\hat{q}\hat{L})}{\hat{q}} \\ &+ \frac{1}{\pi}\int_0^\infty d\hat{q}\ \frac{\sqrt{\hat{q}^2+\kappa^2}}{\sqrt{\hat{q}^2+1}+\varepsilon\sqrt{\hat{q}^2+\kappa^2}}\left[\frac{\sigma}{\hat{q}^2+\kappa^2}-\frac{\varepsilon}{\hat{q}^2+1}\right]\frac{\cos(2\hat{q}\hat{L})}{\sqrt{\hat{q}^2+1}} \\ &- \frac{1}{\pi}\int_0^\infty d\hat{q}\ \frac{\sqrt{\hat{q}^2+1}}{\sqrt{\hat{q}^2+1}+\varepsilon\sqrt{\hat{q}^2+\kappa^2}}\left[\frac{\sigma}{\hat{q}^2+\kappa^2}-\frac{\varepsilon}{\hat{q}^2+1}\right]\frac{\sigma}{\varepsilon}\frac{\cos(2\hat{q}\hat{L})}{\sqrt{\hat{q}^2+\kappa^2}}, \end{aligned} \tag{C2}$$

with the parameters Φ_D, $\Phi_1^{(0)}$, $\hat{L}$, σ, ε, and κ defined as above. It is important to note that, unlike ω_τ^e, ω_τ^s depends on the Donnan potential Φ_D. This is due to the fact that the superposition potential $\Phi_i^s(x,z)$ does not satisfy the boundary condition which relates the electric displacement field at the walls to the surface charge densities. For $\hat{L} \to \infty$, the first, constant, term in Eq. (C2) is cancelled by the leading contribution of the second term. In Eq. (C2) the third and the fourth term go to zero for $\hat{L} \to \infty$. Thus, as expected, in this limit ω_τ^s vanishes. For $\hat{L} \to 0$, the second term vanishes but all other terms remain nonzero. Accordingly, in this limit ω_τ^s reaches a finite nonzero value.

Appendix D: Comparison between the expressions $\omega^e_{\gamma,1}$ and $\omega^s_{\gamma,1}$ for the effective surface interaction

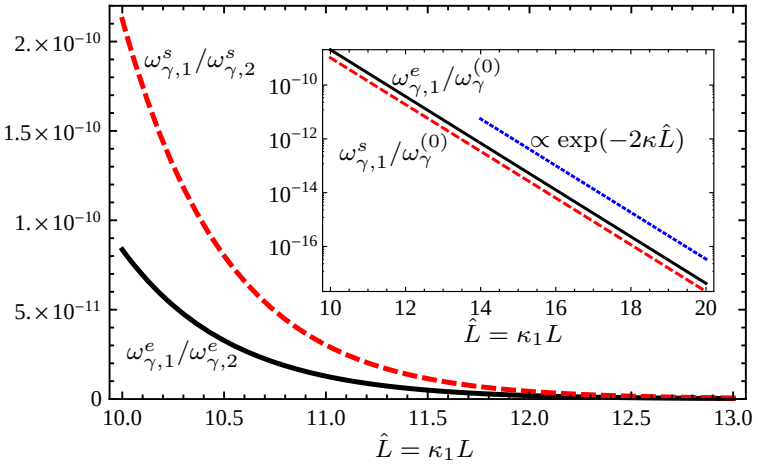

FIG. 6: Comparison between the exact expression (superscript "e", black solid lines, see Eq. (4)) and the superposition approximation (superscript "s", red dashed lines, see Eq. (5)) for the surface interaction energy $\omega_{\gamma,1}(L)$ per total surface area of contact between the walls and medium "1" scaled by $\omega_{\gamma,2}(L)$ for varying $\hat{L} = \kappa_1 L$. Typical experimental values for the parameter ratios $\kappa = \kappa_2/\kappa_1 = 0.025$, $\varepsilon = \varepsilon_2/\varepsilon_1 = 0.025$, and $\sigma = \sigma_2/\sigma_1 = 0.1$ have been chosen for the plots. This data set is the same as the one used for Fig. 2, which displays the behavior of $\omega^e_{\gamma,2}$ and $\omega^s_{\gamma,2}$. Obviously $\omega^e_{\gamma,i}(L)$ and $\omega^s_{\gamma,i}(L)$ differ significantly at small separation distances, but even in the limit of large wall separations the superposition approximation is too small by a factor of 2 (see the offset between the two curves in the inset).

Appendix E: Charge regulation model (In the absence of the interface)

In the context of charge regulation we consider the reaction $AB \rightleftharpoons A^{-q} + B^q$ at the surface of the colloid, where AB is the undissociated surface group which in the presence of the solvent dissociates into a charged surface site A^{-q} and a solvated ion B_q of valency q. We consider the case that B_q is one of the two ion species already present in the bulk electrolyte ($q = q_+ = 1$ if B_q corresponds to the cation and $q = q_- = -1$ if B_q is the anionic species); the corresponding counterions of opposite charge are assumed not to contribute to the regulation of the surface charge. The equilibrium constant K (with the unit 1/volume)

for this reaction is given by

$$K = \frac{[A^{-q}]_s [B^q]_o}{[AB]_s}, \tag{E1}$$

where $[X]_s$ represents the number of species X per surface area and $[Y]_o$ represents the number of species Y per volume in the solution close to the surface [34]. Then the surface charge density of the surface is

$$\sigma_{wi} = -qe[A^{-q}]_s, \tag{E2}$$

the number of surface sites (dissociated plus undissociated) per cross-sectional area is

$$n = [A^{-q}]_s + [AB]_s, \tag{E3}$$

and the number density of ions in the solvent close to the surface is given by

$$[B^q]_o = I + \phi_q(z = \pm L), \tag{E4}$$

where I is the bulk ionic strength (and as such independent of the dissociation reaction at the wall) and $\phi_q(z = \pm L)$ is the deviation close to the surface of the number density of ions of type B from the bulk ionic strength. Since away from the walls the system considered here is homogeneous (due to the absence of the liquid-liquid interface), the quantities $I(\mathbf{r})$ and $\varphi(\mathbf{r})$ in Eq. (B16) are constants. Setting $\varphi(\mathbf{r}) = 0$ without loss of generality, one has $\phi_q(z = \pm L) = -\beta qeI\Phi_p$, where Φ_p is the electrostatic potential at the *p*article surface, i.e., at $z = \pm L$. Using these, the dissociation constant can be written as

$$K = \frac{-\frac{\sigma_{wi}}{qe} I(1 - \beta eq\Phi_p)}{n + \frac{\sigma_{wi}}{qe}}. \tag{E5}$$

In the following we discuss the exact and superposition calculation separately.

1. Exact calculation

In this case, the electrostatic potential at the walls is given by $\Phi_p = \frac{\sigma^e_{wi}}{\kappa_{wi}\varepsilon_{wi}\tanh(\kappa_{wi}L)}$ (see Eqs. (A3) and (A4)). According to Eq. (E5) this implies

$$K = \frac{-\sigma^e_{wi} I \left(1 - \frac{\beta eq\sigma^e_{wi}}{\kappa_{wi}\varepsilon_{wi}\tanh(\kappa_{wi}L)}\right)}{\sigma^e_{wi} + qen}. \tag{E6}$$

Solving this quadratic equation for σ^e_{wi}, one obtains,

$$\sigma^e_{wi} = \frac{\kappa_{wi}\varepsilon_{wi}\tanh(\kappa_{wi}L)}{2\beta eqI}\left(I+K\pm\sqrt{(I+K)^2+\frac{4\beta e^2q^2nIK}{\kappa_{wi}\varepsilon_{wi}\tanh(\kappa_{wi}L)}}\right). \tag{E7}$$

Since $\sigma^e_{wi} \gtrless 0$ for $q \lessgtr 0$ and because the square root is larger than $(I+K)$, the negative sign in front of the square root has to be chosen. Using this and the expression for the inverse Debye length $\kappa^2_{wi} = 2e^2I\beta/\varepsilon$, Eq. (E7) can be further simplified to

$$\sigma^e_{wi} = -\frac{e(I+K)\tanh(\kappa_{wi}L)}{q\kappa_{wi}}\left(\sqrt{1+\frac{2q^2n\kappa_{wi}K}{(I+K)^2\tanh(\kappa_{wi}L)}}-1\right). \tag{E8}$$

For $L \to 0$ this leads to

$$\sigma^e_{wi}(L\to 0) \simeq -\mathrm{sign}(q)e\sqrt{2nKL}. \tag{E9}$$

This is the expression we have used in our discussions. As expected, $|\sigma^e_{wi}(\kappa_{wi}L)|$ decreases upon decreasing L.

2. Superposition calculation

Within the superposition approximation, the electrostatic potential at the *p*article surface is given by $\Phi_p = \frac{\sigma^s_{wi}}{\kappa_{wi}\varepsilon_{wi}}\left(1+e^{-2\kappa_{wi}L}\right)$ (see the first terms in Eqs. (A21) and (A22)) so that according to Eq. (E5)

$$K = \frac{-\sigma^s_{wi}I\left(1-\frac{\beta eq\sigma^s_{wi}\left(1+e^{-2\kappa_{wi}L}\right)}{\kappa_{wi}\varepsilon_{wi}}\right)}{\sigma^s_{wi}+qen}. \tag{E10}$$

Solving this we obtain

$$\sigma^s_{wi} = \frac{\kappa_{wi}\varepsilon_{wi}}{2\beta eqI\left(1+e^{-2\kappa_{wi}L}\right)}\left(I+K\pm\sqrt{(I+K)^2+\frac{4\beta e^2q^2nIK\left(1+e^{-2\kappa_{wi}L}\right)}{\kappa_{wi}\varepsilon_{wi}}}\right). \tag{E11}$$

As in Eq. (E7), in Eq. (E11) the negative sign in front of the square root has to be chosen. For $L \to 0$ this attains a nonzero constant which is at odds with the expected behavior (see Sec. E 1 above). Thus for our discussion, instead of using Eq. (E11), we resort to Eqs. (E8) and (E9) which offer a physically reasonable description of the dependence of the charge density on L.

[1] P. Pieranski, Phys. Rev. Lett. **45**, 569 (1980).

[2] J. D. Joannopoulos, Nature **414**, 257 (2001).

[3] A. D. Dinsmore, M. F. Hsu, M. G. Nikolaides, M. Márquez, A. R. Bausch, and D. A. Weitz, Science **298**, 1006 (2002).

[4] J. C. Loudet, A. M. Alsayed, J. Zhang, and A. G. Yodh, Phys. Rev. Lett. **94**, 018301 (2005).

[5] Q. Chen, S. C. Bae, and S. Granick, Nature **469**, 381 (2011).

[6] Y. Wang, Y. Wang, D. R. Breed, V. N. Manoharan, L. Feng, A. D. Hollingsworth, M. Weck, and D. J. Pine, Nature **491**, 51 (2012).

[7] D. Ershov, J. Sprakel, J. Appel, M. A. Cohen Stuart, and J. van der Gucht, PNAS **110**, 9220 (2013).

[8] X. Mao, Q. Chen, and S. Granick, Nature Materials **12**, 217 (2013).

[9] A. J. Hurd, J. Phys. A **18**, L1055 (1985).

[10] B. J. Park, J. P. Pantina, E. M. Furst, M. Oettel, S. Reynaert, and J. Vermant, Langmuir **24**, 1686 (2008).

[11] R. Aveyard, J. H. Clint, D. Nees, and V. N. Paunov, Langmuir **16**, 1969 (2000).

[12] R. Aveyard, B. P. Binks, J. H. Clint, P. D. I. Fletcher, T. S. Horozov, B. Neumann, V. N. Paunov, J. Annesley, S. W. Botchway, D. Nees, A. W. Parker, A. D. Ward, and A. N. Burgess, Phys. Rev. Lett. **88**, 246102 (2002).

[13] D. Stamou, C. Duschl, and D. Johannsmann, Phys. Rev. E **62**, 5263 (2000).

[14] M. G. Nikolaides, A. R. Bausch, M. F. Hsu, A. D. Dinsmore, M. P. Brenner, C. Gay, and D. A. Weitz, Nature **420**, 299 (2002).

[15] L. Foret and A. Würger, Phys. Rev. Lett. **92**, 058302 (2004).

[16] M. Oettel, A. Domínguez, and S. Dietrich, J. Phys.: Condens. Matter **17**, L337 (2005).

[17] M. Oettel, A. Domínguez, and S. Dietrich, Phys. Rev. E **71**, 051401 (2005).

[18] A. Würger and L. Foret, J. Phys. Chem. B **109**, 16435 (2005).

[19] A. Domínguez, M. Oettel, and S. Dietrich, J. Chem. Phys. **127**, 204706 (2007).

[20] A. He, K. Nguyen, and S. Mandre, EPL **102**, 38001 (2013).

[21] A. Domínguez, D. Frydel, and M. Oettel, Phys. Rev. E **77**, 020401(R), (2008).

[22] A. D. Law, M. Auriol, D. Smith, T. S. Horozov, and D. M. A. Buzza, Phys. Rev. Lett. **110**, 138301 (2013).

[23] W. Russel, D. Saville, and W. Schowalter, *Colloidal Dispersions* (Cambridge University Press, Cambridge, 1989).

[24] K. Masschaele, B. J. Park, E. M. Furst, J. Fransaer, and J. Vermant, Phys. Rev. Lett. **105**, 048303 (2010).

[25] M. Bier, A. Gambassi, and S. Dietrich, J. Chem. Phys. **137**, 034504 (2012).

[26] F. H. Stillinger, Jr., J. Chem. Phys. **35**, 1584 (1961).

[27] V. S. Bagotsky, *Fundamentals of electrochemistry* (Wiley, Hoboken NJ, 2006).

[28] M. Bier, J. Zwanikken, and R. van Roij, Phys. Rev. Lett. **101**, 046104 (2008).

[29] K. A. Danov, P. A. Kralchevsky, and M. P. Boneva, Langmuir **20**, 6139 (2004).

[30] W. Chen, S. Tan, Y. Zhou, T.-K. Ng, W. T. Ford, and P. Tong, Phys. Rev. E **79**, 041403 (2009).

[31] R. Kesavamoorthy, C. B. Rao, and B. Raj, J. Phys.: Condens. Matter **5**, 8805 (1993).

[32] I. S. Gradshteyn, and I. M. Ryzhik, *Table of Integrals, Series, and Products*, 6th ed. (Academic, San Diego, 2000).

[33] I. Ibagon, M. Bier, and S. Dietrich, J. Chem. Phys. **138**, 214703 (2013).

[34] As we are considering only length scales larger than the bulk correlation length, $[Y]_o$ is obtained from the actual microscopic number density profile upon coarse graining, i.e., by averaging out its spatial variations at wavelengths up to the bulk correlation length.